JOURNAL OF Materials CHEMISTRY
Feature Article

Fullerene architectures made to order; biomimetic motifs — design and features

Dirk M. Guldi*[a] and Nazario Martín[b]

[a]*Radiation Laboratory University of Notre Dame, Notre Dame, USA IN 46556. E-mail: guldi.1@nd.edu*
[b]*Departamento de Química Orgánica, Facultad de Ciencias Químicas, Universidad Complutense, Madrid, Spain E-28040*

Received 28th February 2002, Accepted 7th April 2002
First published as an Advance Article on the web 31st May 2002

This article highlights the progress made in the design, synthesis and study of supramolecular fullerene architectures that are based upon biomimetic organization principles. In particular, an overview of hydrogen-bonding, π–π stacking, metal-mediated complexation and electrostatic motifs is given, which have been used to incorporate fullerenes into well-ordered arrays. Owing to the presence of fullerenes, as an integrative building block, the majority of the presented molecular assemblies exhibit unique and remarkable features. Issues relevant to electron-donor–electron-acceptor interactions are considered.

Introduction

In nature both covalently-bonded and self-assembled motifs are widely spread organization principles that regulate size, shape and function down to the nanometer scale.[1] Exceptional and aesthetical illustrations for the sophistication of this course are protein shells — including those of the photosynthetic reaction center — with highly complex performances such as energy storage, protection and transport of inorganic or organic molecules.[2] The ability to engineer extended 1D, 2D, or 3D architectures at the molecular level, by modifying individual chemical building blocks, sparks a very active field.

Unquestionably, the weak molecular interactions, as found in natural donor–acceptor ensembles, bears a deep fascination as a superior means to control (*i*) the organization of photo- and redox-active components and (*ii*) their mutual, electronic coupling. Stimulated by this vision and considering the significant relevance to natural photosynthetic events, substantial efforts are devoted to the development of non-covalent linkages, associating the requisite donor and acceptor.[3] In light of all this, self-assembly, molecular recognition and inclusion phenomena emerged as meaningful assets in devising supramolecular architectures. Since the key steps — either spontaneous or chemically induced — are often thermodynamically driven processes, the yields of self-assembled ensembles are likely to exceed those involving the formation of covalent bonds.

In principal, a variety of biomimetic methodologies, such as hydrogen-bonding, π–π stacking, metal-mediated complexation and electrostatic interactions, are potentially useful promoters to engineer stabilized large arrays.[4] They all guarantee to control the integration in donor–acceptor composites and to achieve predetermined architectures of controlled sizes and outer-shell structures, with high directionality and selectivity. A central benefit of these biomimetic motifs is that they are reversible, and, in contrast to truly covalent bonds, their binding energies are highly dependent on the chemical environment and temperature. Frequently, biomimetic-driven processes are also composed by templating the host architecture around molecular or ionic guests.[5]

Certainly, one of the major challenges that still lies ahead of us is to regulate the weak forces, on a molecular basis, which will dictate, at the end, size and shape in relation to function of the resulting composite. Can molecular tailoring of, for example, fullerenes, which are rigid, conformationally restricted scaffolds, contribute to the induction of completely different kinds of assemblies? Owing to the spectacular advances in the chemistry of fullerenes,[6] remarkable progress has been made in non-covalently bonded structures, in solutions and in crystals, which shall be highlighted in this review. The incentive shall always be the critical perspective of potential electron-donor–electron-acceptor interactions.

Hydrogen bonding motifs

Hydrogen bonding is recognized as a fundamental means in defining the 3D structure of chemical and biological systems.[7] In fact, among the many biomimetic methodologies only the hydrogen bonding motif meets the criteria of high directionality and selectivity. Its main limitation is the insufficient stability. This can be overcome by the presence of an array of highly directional multiple hydrogen bonds. Multiple hydrogen bonding, for example, has been successfully applied for the preparation of very stable complexes in different areas.[8] A remarkable stable dimer ($K_a > 10^6$ M^{-1}) was prepared from 2-ureido-4-pyrimidone derivatives, *via* a self-complementary muster of four hydrogen bonds. Alternatively, the combination with other non-covalent forces — electrostatic or hydrophobic interactions — emerged to self-organize ensembles with a much increased stability.

Although fullerenes have been used frequently as a building block in the preparation of supramolecular systems,[9] only recently have a few examples been reported, in which hydrogen bonding motifs dictate the ensemble arrangement. One of the first examples, screening the formation of a self-assembled monolayer (SAM), was carried out by self-assembly of fullerenes, endowed with a monobenzo-18-crown-6 ether moiety on a gold surface (*vide infra*).[10]

More recently, the synthesis of a C_{60}-dimer followed — Scheme 1. Specifically, a C_{60}–dibenzylammonium adduct was threaded through the cavity of a crown ether macrocycle in C_{60}–dibenzo-24-crown-8.[11] In this case, hydrogen bonding and ion–dipole interactions are responsible for the formation of the first supramolecular C_{60}-dimer. The latter exhibits an association constant of 970 M^{-1}. In a similar way, Scheme 2

 DOI: 10.1039/b203007a

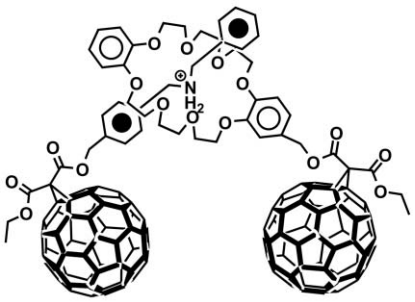

Scheme 1 A supramolecular C_{60}-dimer; C_{60}–dibenzylammonium/C_{60}–dibenzo-24-crown-8.

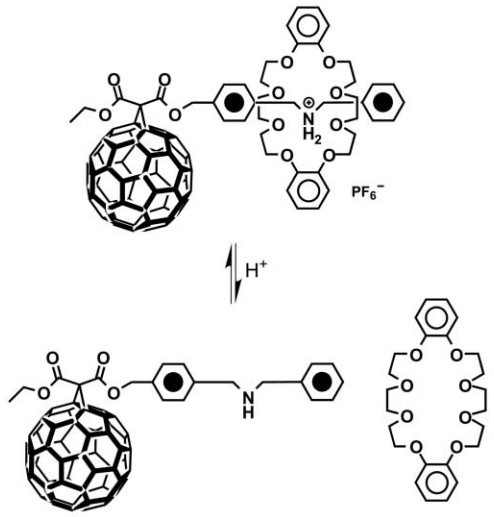

Scheme 2 A reversible acid–base controlled de-/rethreading process of a C_{60}–dibenzylammonium conjugate and dibenzo-24-crown-8.

illustrates that the C_{60}–dibenzylammonium conjugate threads reversibly through the cavity of dibenzo-24-crown-8 to form a 1 : 1 complex with a pseudorotaxane-like geometry (K_a = 1.25 × 10^4 M^{-1}). Interestingly, when dibenzo-24-crown-8 is complexed to the C_{60}–dibenzylammonium conjugate, the luminescence associated with the catechol rings of the crown ether was partially quenched.

Slightly different is the approach that we reported on the synthesis of the first rigid non-covalent C_{60}-dimer, in which both molecular subunits are linked by a self-complementary array of hydrogen bonding — donor–donor–acceptor–acceptor.[12] The selected four-point hydrogen motif, based on a 2-ureido-4-pyrimidone moiety guarantees the molecular recognition in solution and leads to a unique non-covalent model system. In a related C_{60}-dimer system, the 2-ureido-4-pyrimidone moiety was connected to the C_{60} core through a cyclopropane ring.[13]

The electrochemical studies on these C_{60}-dimers indicated that both C_{60} moieties are reduced simultaneously. This observation, in conjunction with the spectroscopic characterization, supports the critical notion that there is in the ground state little, if any, electronic interaction between the individual C_{60} subunits. In the excited state, the singlet excited state of the C_{60}-dimer is subject to an accelerated deactivation, resembling the trend seen for a covalently bridged C_{60}–C_{60} molecule. Upon adding protic solvents — ethanol, trifluoroethanol and hexafluoroisopropanol — to a CH_2Cl_2 solution, a progressive enhancement of the fullerene fluorescence was observed, reaching in the most protic solvent — hexafluoroisopropanol — a quantum yield similar to that observed for the reference 2′,5′-dihydro-1′*H*-fulleropyrrolidine. Therefore, photochemical means bear a great potential, not only to distinguish between a

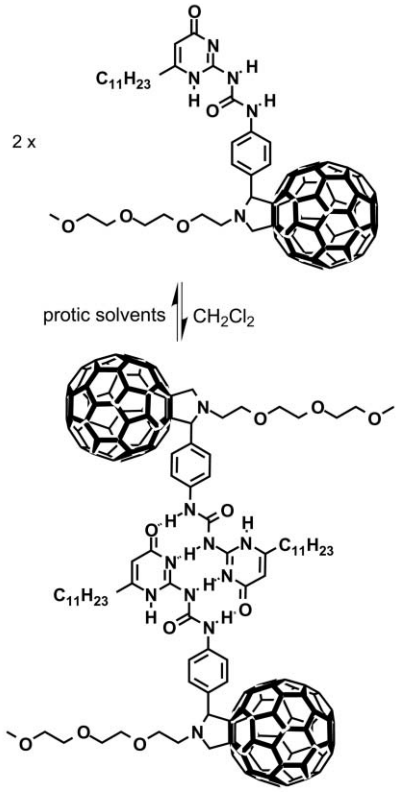

Scheme 3 A supramolecular C_{60}-dimer linked by a self-complementary array of hydrogen bonding — donor–donor–acceptor–acceptor.

monomer and dimer, but also to monitor the gradual destruction of the hydrogen bonding motif, which stems from adding hydrogen bond disrupting solvents, shown in Scheme 3.

No doubt, hydrogen bonding motifs confer outstanding benefits for constructing photo- and electroactive donor–acceptor models. Studies performed with biomimetic model systems, wherein donor and acceptor molecules are tethered together non-covalently *via* hydrogen bonds, have shown that the electronic coupling through hydrogen bonds may, in fact, be larger than those mediated by either σ- or π-bonding networks. These findings pave the way for the preparation of novel C_{60}-based donor–acceptor systems, in which the electronic interaction of the C_{60} core with the electron donor unit will take place through a well-designed network of hydrogen bonding.

π-Stack motifs

π-Stacking implements the weak interactions between electron rich and electron poor aromatic rings. The attractive interactions are hereby proportional to the contact surface area of the two π-systems and the relative orientation of the two interacting molecules, which is determined by the electrostatic repulsions between the two negatively charged π-systems.[3]

One of the central concepts, reasoning the composition of 3D fullerene structures, is the introduction of five-membered (pentagons) rings, which are primarily responsible for their convex curvature.[14] They function like defects in a graphite structure, which governs the non-planarity of the fullerene's π-electronic arrangement. This structural topic also imposes a number of electronic consequences. Most importantly, they generate alternating areas of electron-richness and electron-deficiency in C_{60}, which correspond to the hexagon and pentagon faces, respectively. Overall an anisotropic electron distribution is thereby created. This is then the basis for

predetermined interactions with substrates.[15] Depending on the electronic nature of the substrate the ambivalent structure of C_{60} can adapt and associate by maximizing the electronic/spatial overlap. Thus, fullerenes exhibit much higher tendencies to interact with other molecules than what is typically found for conventional 2D organic molecules.

Concave–convex

Matching a concave surface to the convex shape of C_{60} is one means to gain control over the inherently weak association between a host moiety and a molecular guest. The synopses of in-built shape- and size-specific receptor sites are two-fold: firstly, it ensures the efficient binding. Secondly, it exerts a major challenge to find the right match. Prominent instances are nano-sized, bowl-shaped molecules or container molecules with curved, open-ended cavities, such as cyclodextrins,[16] benzotri(benzonorbornadienes),[17] calixarenes,[18] calixnaphthalenes[19] and cyclotriveratrylene.[20] They all form remarkably stable composites with fullerenes, which exhibit high guest selectivity and control of reactivity.

Cyclodextrins

Cyclodextrins — alpha (α), beta (β) and gamma (γ) — are rigid, cyclic oligosaccharides with well-defined hydrophobic cavities.[16] Considering the right balance between cavity radius and fullerene size leads to the assumption that γ-CD should be the only candidate to host C_{60}. Nevertheless, molecular modeling suggests that a full incorporation — even in the form of a 1 : 1 complex — is practically impossible to achieve. Despite this apparent size mismatch, an incorporation of a single C_{60} molecule between the cavities of two γ-cyclodextrin molecules — in the form of a 2 : 1 complex (Scheme 4) — has been postulated and later confirmed. In fact, it produces the most stable solutions, independent of the method of preparation, with C_{60} concentrations as high as 1.4×10^{-3} M.[16i]

One particular study on C_{60}–γ-CD should be highlighted, due to its far-reaching significance in employing C_{60} as an electron acceptor.[21] Under anaerobic conditions the singly reduced $C_{60}^{\bullet-}$–γ-CD — formed in radiolytic or photolytic experiments — is quite stable. Variation of the pH, by addition of acid or base, had a significant impact on the stability and also on the yield of the diagnostic $C_{60}^{\bullet-}$–γ-CD absorption band at 1080 nm.[21d] A semilogarithmic correlation between the proton concentration and the intensity of the fullerene π-radical anion band is observed in anaerobic aqueous solutions. This observation has been ascribed to a reversible protonation of $C_{60}^{\bullet-}$–γ-CD to afford $C_{60}H^{\bullet}$–γ-CD. Experimental proof for this assumption was brought forward by the fact that the 1080 nm absorption, in an alkaline solution (pH 10), diminished upon acidifying (pH 3) and was completely restored upon subsequent addition of base (pH 10). The reversible protonation process gives rise to a pK_a of 4.5.

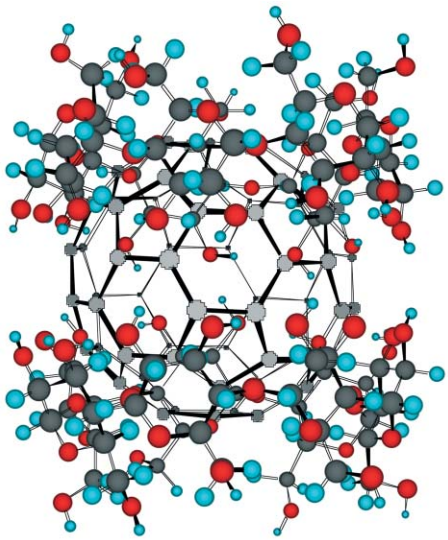

Scheme 4 Schematic illustration of a γ-cyclodextrin–C_{60} encapsulate — in the form of a 2 : 1 complex.

Calixarenes

Unlike the aforementioned class of containers, the structures of calixarenes[18] allow for some more structural flexibility, which plays a considerable part in their affinity to bind C_{60}. Support for this view was lent from a comparison of the optical-active modes in the vibrational spectrum of the C_{60}–*p*-*t*Bu-calix[8]-arene complex with those of the empty *p*-*t*Bu-calix[8]arene.[22] Also ^{13}C-NMR signals suggest complexation-induced conformational changes of the calixarene host: a two-winged or alternate conformation, with the 1 and 5 phenolic units "out" and "down", is most likely present.[23] Typical association constants for C_{60}–calixarenes ensembles in toluene range between 35 M^{-1} for *p*-*t*Bu-hexahomooxacalix[3]arene[24] and 1.66×10^4 M^{-1} for octamethoxy-*p*-*t*Bu-calix[8]arene.[18n]

A more detailed examination with calix[4]arene, homooxacalix[3]arene, calix[5]arene, calix[6]arene and calix[8]arene in toluene supports the fact that only those calix[*n*]arenes can include C_{60}, that hold a well-preorganized cone cavity.[24,25] Just homooxacalix[3]arene ($K = 35 \pm 5$ M^{-1}), calix[5]arene ($K = 330 \pm 10$ M^{-1}) and calix[6]arene ($K = 87 \pm 5$ M^{-1}) meet this requirements, that is, a cone configuration and a benzene ring inclination suitable for a multi-point interaction with C_{60}. This is illustrated in Scheme 5.

Inclination of the benzene rings and cavity of the molecular hosts are not the sole factors regulating the binding affinity, a similarly strong impact was noted upon varying temperature and/or solvent. Increasing the temperature from 294 to 315 K led to smaller binding constants, with differences as large as two orders of magnitude.[18n] As far as the medium is concerned, benzene and toluene are generally found to yield the highest association constants, while variations of up to 10 were found in CS_2, CCl_4, *o*-dichlorobenzene and *o*-xylene.[18e,g,n] Thus, the association strength increases with decreasing the overall solubility of C_{60}, reflecting the competition between complex formation and solvation of the guest. In general the binding affinity for C_{60} is larger than for C_{70}, with the actual difference depending largely on the aforementioned factors: host cavity, solvent and temperature.

Quite interestingly, the intensity of the narrow and broad line width of the EPR signals decreased, when $C_{60}^{\bullet-}$ was electrochemically generated in the presence of the complexing *p*-benzylcalix[5]arene.[26] This indicates that the π–π interactions were sufficiently strong to alter the EPR signals of $C_{60}^{\bullet-}$.

One of the water soluble complexes, namely, C_{60}–homooxocalix[3]arene was subject to fluorescence and transient absorption measurements in aqueous media, following visible light excitation.[27,28] Very dramatic effects were noted in

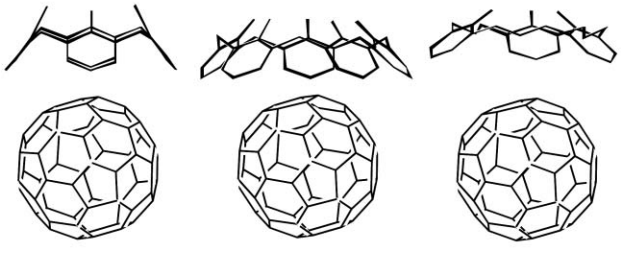

Scheme 5 Interaction of calix[4]arene, calix[5]arene and homooxacalix[3]arene with C_{60}, only calix[5]arene and homooxacalix[3]arene can provide a benzene ring inclination suitable to bind C_{60}.

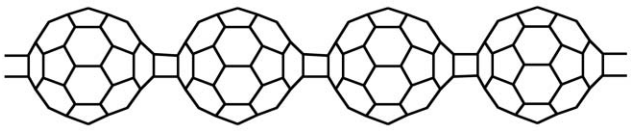

Scheme 6 Schematic illustration of the strictly [2 + 2] addition polymer of C_{60}.

comparison to C_{60} benzene and C_{60}–γ-CD aqueous solutions: blue-shifted fluorescence (*i.e.*, from 700 nm to 531 nm) and blue-shifted transient triplet maxima (*i.e.*, from 750 nm to 545 nm) diagnose an electronic perturbation within the C_{60}–homooxocalix[3]arene inclusion complex.

As C_{60} is particularly prone to co-crystallization with other molecules, the organization of the co-crystallizing components becomes useful for further refinement of the solid-state morphology.[29] One of the systems, that is, C_{60} with *p*-bromocalix[4]arene propyl ether co-crystallizes in strictly linear, separated columns. Applying heat and pressure to these linear columns, the C_{60}–bromocalix[4]arene propyl ether co-crystal transformed into a linear [2 + 2] addition polymer (Scheme 6), without showing any evidence for notable cross-linking products. Upon photopolymerization of a pristine C_{60} sample, at least three polymer phases are reported with characteristics ranging from those of rhombohedral and orthorhombic to tetragonal phases.[30] In retrospect, this elegant demonstration offers new stimuli in the field of crystal engineering.

Calixnaphthalenes

Probably, the most important structural disparity between calixarenes and the closely related calixnaphthalenes is that the latter are a class of cavitands possessing deeper cavities.[19] The extra fused aromatic rings on each naphthalene unit allow better contacts between host and guest and deeper penetration of the latter. This effects their complexation properties with values of 3.0×10^2 M^{-1} and 7.08×10^2 M^{-1} for *p*-*t*Bu-hexahomotrioxacalix[3]naphthalenes and *t*Bu-calix[4]naphthalenes, recognizably larger than for the calixarene analogs. The binding affinities in the different solvents were opposite to the trends reported for calixarenes — the binding for calixnaphthalenes in CS_2 is actually higher than in toluene or benzene. A detailed thermodynamic study reveals that both solvophobic effects (*i.e.*, a larger number of CS_2 molecules are displaced from the cavitand cavity upon C_{60} binding) and π–π interactions are cooperative driving forces for the complexation processes.[19b]

Resorcarene

A wider synthetic flexibility is definitely given in the application of resorcarene-based materials to stabilize C_{60} within their framework.[31] In particular, metal ions in conjunction with multiple units of a dithiocarbamate-resorcarene ligand are suited to device resorcarene-based nanostructures, whose geometries can be varied by the choice of metal ions and their oxidation states. In case of cadmium and zinc, the resulting trimeric networks (see Scheme 7) were shown to encapsulate C_{60} with binding constants ranging from 2.9×10^4 M^{-1} to 1.2×10^5 M^{-1} in toluene and slightly larger values in benzene. The intramolecular distances, separating the opposing metal centers from each other are on the order of 14.7 Å. Importantly, in a copper-based tetrameric network, in which four ligands are placed at the apices of a distorted tetrahedron, distances across the tetrahedron can reach as high as 20.4 Å. In principal, the larger size of the cavity should facilitate the encapsulation of higher fullerenes as well.

In retrospect, donor–acceptor interactions between the π-electron rich aromatic rings and the π-electron deficient

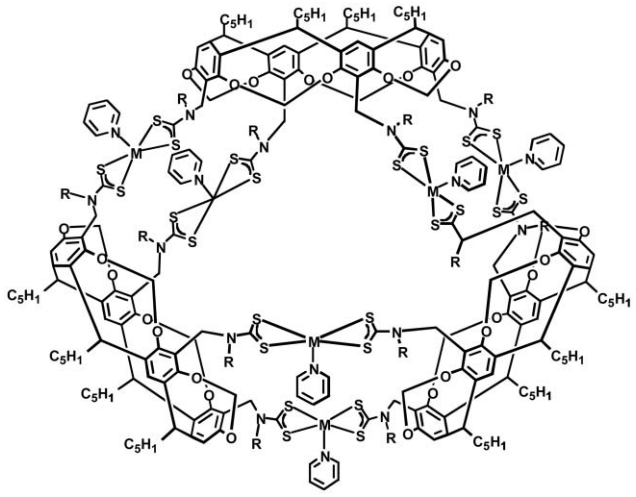

Scheme 7 A resorcarene-based host architecture to bind C_{60} (M = Cd or Zn).

domains of C_{60}, together with van der Waals forces, provide the major stabilization for the solution complexes. While the complementary curvature of the interacting species maximizes the number of intermolecular contacts, formation of these concave–convex composites are entropically disfavored due to a more ordered state. The above outlined examples manifest that a broader applicability of a given nanostructure comes only at a price of an inferior selectivity. Notably, a mismatch in size generally results in the spontaneous and irreversible formation of aggregates, resembling the cluster phenomena of C_{60} in polar and aqueous media (*vide infra*) or even upon aging of surfactant-capped C_{60} solutions.[32] Scattered reports support this hypothesis. The *p*-*t*Bu-calix[8]arene complex of C_{60}, for example, exists in a stable configuration only in the solid state, while upon solubilization it dissociates into the free components or micelle-like composites with a trimeric cluster that is surrounded by three host molecules in a double cone formation.[33] Not unexpectedly, aggregation phenomena are also observed in the C_{60}–cyclotriveratrylene case, leading to a polymeric zigzag array of C_{60} in the solid state, each in the cavity of a cyclotriveratrylene molecule.[34] It is important to note that cluster or aggregates are ineffective probes for photoinduced electron transfer examinations, since the close packing expedites excited state deactivation processes.

Planar–convex

A fascinating and widely applicable scenario involves the utilization of strong π–π associations between π-electron rich macrocycles, in general, and fullerenes as a means to engineer supramolecular nanoarrays with remarkable photoactive and magnetic properties.

The first X-ray crystal structure involving a fulleropyrrolidine, H_2P–C_{60} (H_2P = free base tetraphenylporphyrin), which was grown as a chloroform solvate, started this very exciting field.[35] The crystal packing gives way to a clear picture on the disposition of both moieties.[35b] An appreciable intermolecular interaction evolves from an unexpectedly close approach between C_{60} and the porphyrin. The distances of the closest C_{60} C-atoms to the mean plane of the inner core of the porphyrin are, with values of 2.78 Å and 2.79 Å, quite short. In this context, the inter-layer separation in graphite (3.35 Å) and the interfacial porphyrin–porphyrin separations (> 3.2 Å) may be viewed as good reference points. As a consequence, a new donor–acceptor relationship was formulated, that is, augmentation of the usual π–π association by electron donor–electron acceptor interactions.

Following the remarkable results of the initial work on H_2P–C_{60},[35b] this aspect was systematically explored in a series

of MP–C_{60} cocrystallates (*i.e.*, MP stands for metalloporphyrin).[36] Various metal species, ranging from Mn, Co, Ni, Cu, Zn to Fe, were chosen. Favorable van der Waals attractions between the convex π-surface of C_{60} or C_{70} and the planar π-surface of MP, assist in the supramolecular recognition, overcoming, however, the necessity of matching a concave-shaped host with a convex-shaped guest structure (*vide supra*). Common to all C_{60}-based assemblies is that electron rich areas, namely, carbon atoms at hexagon–hexagon junctions, lie over the center of the porphyrin ring. C_{70}, on the other hand, adapts a configuration that brings the poles of the ellipsoidal framework — again carbon atoms located at the intersection of hexagon faces — into contact with the porphyrin. As a direct consequence, complexes with unusually short contacts (2.7–3.0 Å), shorter than ordinary van der Waals contacts (3.0–3.5 Å), are formed. This shows that MP–C_{60} associative forces constitute an important organization principle. A wide variety of crystal structures were found; honeycomb motifs, puckered graphite-like layers, zigzag-chains and columns.[36]

Besides porphyrins, cocrystallites of C_{60} were also found with porphyrazines,[37] as another representative of the diverse family of π-extended macrocyclic complexes.[38] They reveal interesting supramolecular structures: While, for copper(II) a C_I-symmetric sandwich complex of two slightly dished porphyrazines units enclosing one C_{60} was found, nickel(II) features a non-centrosymmetric 1 : 1 complex with a strongly wrapped porphyrazine unit (Scheme 8). Again, strong π–π associations are believed to promote these remarkable ordering principles.

In concentrated toluene solutions the following picture develops. For example, when millimolar concentrations of MP and C_{60} are either titrated or spontaneously mixed, ^{13}C- and ^{1}H-NMR studies reveal mutually upfield shifts, which is a clear indication for the presence of complex formation. Absorption spectroscopy, on the other hand, proved to be insensitive to detect appreciable MP–C_{60} interactions, which may lead to the false presumption that the degree of MP–C_{60} association might be weak.

In very dilute solution conditions — micromolar to be exact — MP–C_{60} interactions are also inferred on the following grounds.[39] The rate constants for electron transfer from various MP π-radical anions (M = Zn, In, Ge, Al, Ga, Sn, Sb) to C_{60} are found to be in the range of (1–3) × 10^9 M^{-1} s^{-1}, which corresponds to nearly diffusion-controlled processes. The lack of dependence, despite the large variation in one-electron reduction potentials for the examined MPs might reflect the fact that the investigated MPs and C_{60} experience already electronic interactions in the ground state. Again, no perturbation of the ground state transitions was detectable. Truly, the absorption spectrum appears simply as a good superimposition of the two different components, that is,

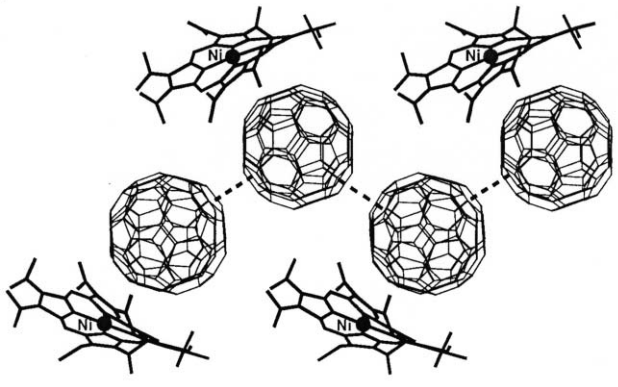

Scheme 8 Part of the continuous zigzag chains of π-stacked nickel(II) porphyrazine–C_{60} cocrystallites.

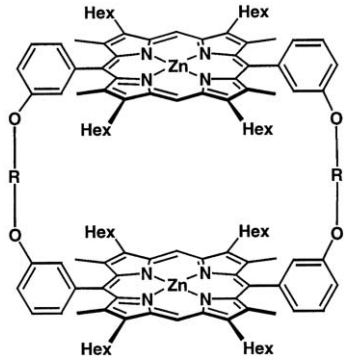

Scheme 9 A metalloporphyrin "cyclic-dimer" host (*i.e.*, ZnP) to bind C_{60}; R = $(CH_2)_6$ or $CH_2C{\equiv}C{-}C{\equiv}CCH_2$.

MP and C_{60}, reflecting the data gathered in the millimolar regime.

Complementary sizes and maximizing the number of points of interactions are key factors in devising stable fullerene architectures, at least in the absence of alternative motifs such as hydrogen bonding, electrostatic and metal coordination. The control over the competition between host–host, guest–host and host–host interactions, which is particularly evident in fullerene chemistry where, for example, C_{60}–C_{60} interactions play a major role, is important in determining the structure of supramolecular ensembles. Thus, following similar incentives, a porphyrin "cyclic-dimer"[40] and a porphyrin "jaw",[41] depicted in Schemes 9 and 10, respectively, were developed. The electron-rich walls of the porphyrins and their considerable contact with incumbent C_{60} encouraged experiments, and strong interactions were indeed detected. In both constructs, discrete van der Waals complexes are realized with a core of two porphyrins (*i.e.*, PdP (palladium 3-pyridyltriphenylporphyrin)[41] or ZnP (zinc biphenyltetrahexylporphyrin)[40a]) controlling the selective C_{60} incorporation.

The close proximity of the MP and C_{60} π-systems in the "cyclic-dimer" and "jaw" gives rise to π-electronic donor–acceptor interactions, whose effects are detectable in the shifts of the absorption bands in the spectra of the resulting composites. In comparison to the model porphyrin systems, red shifts of the Soret and *Q*-band transitions, accompanied by lower extinction coefficients, are consistently observed and attest to the mutual perturbation of the π-systems. Concomitantly, the chromophore's emission gives rise to a progressive quenching after addition of variable C_{60} concentrations.

Based on metal-to-fullerene-charge-transfer interactions an unprecedented high association constant for binding C_{60} of 2.4 × 10^7 M^{-1} was reported for the "cyclic-dimer".[40b] Notably weaker is, however, the interaction between the two PdP in the

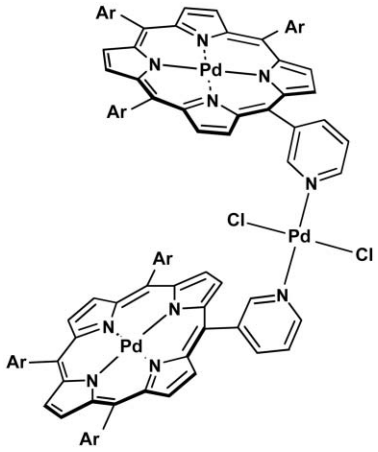

Scheme 10 A metalloporphyrin "jaw" (*i.e.*, PdP) to bind C_{60}.

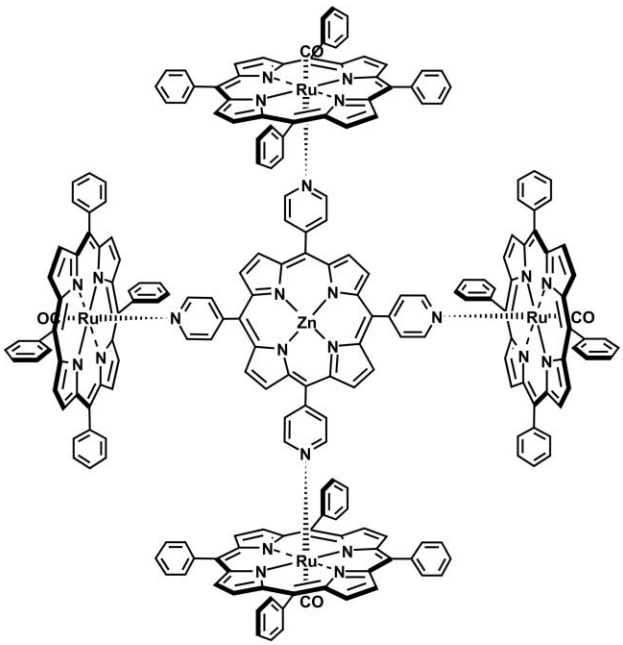

Scheme 11 Self assembly of a ZnP(4)–$(RuP)_4$ box.

porphyrin "jaw", for which an association constant of 7×10^5 M^{-1} was determined. The difference in association rates can be rationalized in terms of the flexible framework of the "cyclic-dimer", which ensures perfect encapsulation. For example, X-ray crystallographic measurements reveal in the C_{60}-"cyclic-dimer" complex shortest zinc–carbon distances of 2.765 and 2.918 Å, notably shorter than the sum of the van der Waals radii (3.09 Å). In addition, the hexamethylene spacers are folded and the ZnP's planarity is slightly distorted to maximize the π-overlap with the convex C_{60} surface. Upon precluding the flexibility, by using a rigid diacetylenic spacer instead of the hexamethylene spacer, no complex association was found at all.

To ensure strong association constants in combination with well-defined geometries, a multi-point interaction approach was described in the form of a self-assembled porphyrin "box" (*i.e.,* four side wall ruthenium porphyrins, RuP, and one central zinc porphyrin, ZnP) — Scheme 11.[42] The large area of contact should in principle lead to diminished C_{60}–C_{60} interactions and indeed this was found to be the case. It was demonstrated that these systems are useful for expediting the supramolecular interactions of the porphyrins with a suitable C_{60} electron acceptor at the molecular level. Furthermore the systematic variation of the geometry, namely, straight *versus* tilted facilitated or hindered the incorporation of a 3D C_{60} moiety into an ensemble, constituted by 4 side-wall RuP and 1 central ZnP. The assignments are based, in large, on a detailed photophysical investigation, especially focusing on the steady-state emission of the ZnP (*i.e.*, fluorescence) and the RuP (*i.e.*, phosphorescence).

A different approach towards supramolecular nanoarchitectures is the use of polybenzyl ether dendrimers that complex C_{60} within the interior core.[43] A meso-tetraphenylporphyrin core provides a correctly sized space for C_{60} inclusion. The expected decrease of the Soret-band was seen in the presence of C_{60}, but without the obligatory red-shift of the transition. Based on the poor solubility, determination of the association constant could not be performed. However, comparing the different dendrimer generations gave rise to the following conclusions: Firstly, the dendritic branches are crucial to provide the important complexation. Secondly, C_{60} is in the close vicinity of the meso-tetraphenylporphyrin core.[44]

In conclusion, the utilization of topological controlled π–π associations between C_{60} and metalloporphyrins constitute an important organization principle: whenever affirmed by the molecular topology of the system, these moieties give rise to selective supramolecular interactions. Since the resulting ensembles have a truly noncovalent character they mimic well-arranged organic pigments (*i.e.*, light harvesting antenna ensemble and photosynthetic reaction center (PRC)) and other cofactors.

Convex–convex

An agonizing feature of pristine C_{60} is that this carbon allotrope proves to be virtually insoluble in aqueous environments. In fact, aggregation/clustering transforms the convex spheres in polar solvents into hierarchical mesoscopic structures.[45–61] A fundamental and imperative challenge is to gain control over the cluster size, which has led to two different strategies. The first one implements the rapid injection of a polar — non-fullerene-like — solvent (*i.e.*, acetonitrile or water) into a non-polar solution of the respective C_{60}, C_{70}, *etc.* (*i.e.*, toluene or THF).[45–54] In an alternative approach, a dispersion of a hydrophobic fullerene sample, which carries, for example, a hydrophilic ammonium group in distilled and filtered water or acetone was immersed in an ultrasonic bath for several time intervals.[55–59]

Clusters in polar solutions

In accord with the first approach, C_{60}- and C_{70}-clusters were generated in a room temperature toluene–acetonitrile solvent mixture.[45] Solvatochromic changes served as good indicators for cluster formation. In the case of C_{70}, the color changed from orange to reddish purple, while C_{60}-clusters exhibited a brownish yellow color. The latter is strikingly different from the magenta solution of a C_{60}-monomer. After all, decreasing the acetonitrile composition changes the solution color and absorption spectrum back to those of the corresponding monomers. Photon correlated spectroscopy of quasi-elastic light scattering showed that the average size of the clusters is 186 nm for C_{70}, while for C_{60} they fall in the relatively wide range of 140 to 270 nm. The large variation of the C_{60}-cluster sizes were correlated with the initial C_{60} concentration (5.0×10^{-6}–1.0×10^{-4} M) and the toluene–acetonitrile composition (40–90%). All cluster suspensions are stable, showing no sign of precipitation over time.

Using water as an additive to THF solutions of C_{60} and C_{70}, fairly monodisperse clusters are observed, whose diameters agree well with the average hydrodynamic diameter obtained by dynamic light scattering.[46] In particularly, values of 62.8 nm for C_{60} and 63.0 nm for C_{70}, are significantly smaller than the values reported previously for fullerene dispersions in water (*i.e.*, mean diameter of 300 nm) and those in toluene–acetonitrile (*i.e.*, mean diameter of 300 nm).[47] The electrostatic repulsion between the similarly charged clusters is believed to be important for the stability of the dispersions.[48]

Importantly, photophysical examinations of 270 nm large C_{60}-clusters in ethanol[49] reveal that the triplet excited state decays rapidly within 50 ns after the laser pulse, corroborating data recorded with, for example, an amphiphilic *N,N*-dimethylfulleropyrrolidinium in aqueous media.[50] The lifetime of the triplet excited state is very sensitive to the environment and in closely packed clusters becomes subject to an efficient triplet–triplet annihilation. As a reference point, the monomeric analogue, either surfactant capped or dissolved in an organic solvent, gives rise to lifetimes of several tens to a hundred of microseconds.

Relatively large clusters were also generated from 1,2,5-triphenylfulleropyrrolidine in toluene–acetonitrile (1 : 3 *v*/*v*).[51] The mean diameter is 180 nm, as derived from dynamic light scattering. Surprisingly, electron transfer quenching rates of the triplet excited state ($\tau = 2$ μs) with ferrocene,

N-methylphenothiazine and *N,N*-dimethyl-*p*-anisidine were found to be several orders of magnitude faster than that of the monomeric analogue, which are in the range of diffusion-controlled limits. This is attributed to the entrapment of donor molecules within the porous cluster network. Forces stemming from the hydrophobicity of the *N*-methylphenothiazine donor are also likely to expedite the electron-transfer interaction. Similarly, a mean diameter of ~170 nm was found for C_{60}–aniline clusters in toluene–acetonitrile (1 : 3 *v*/*v*).[52] For photovoltaic applications these C_{60}–aniline clusters were deposited on nanostructured SnO_2 electrodes under an electric field.[53] At low applied DC voltages (*i.e.*, < 5 V) C_{60}–aniline clusters in toluene–acetonitrile (1 : 3 *v*/*v*) grow in size from 160 nm to ~200 nm, while at higher voltages (*i.e.*, 50 V) they are deposited onto the electrode as thin films.[53a] The resulting nanostructured films reveal relatively large photocurrents with a photoconversion efficiency of 3–4%, when employed as photoanodes in photoelectrochemical cells.

17 nm sized, globular particles, by far the smallest spheres detected so far, were seen by AFM and dynamic light scattering measurements upon addition of water to a THF solution of a potassium salt of pentaphenylated C_{60} ($Ph_5C_{60}K$).[54] The resulting anion, $Ph_5C_{60}^-$, associates into spherical bilayers.

Clusters upon sonication

The first report on ultrasonication appeared in the context of treating a *N,N*-dimethylfulleropyrrolidinium salt in an aqueous solution.[57] Representative TEM images clearly reveal perfectly round shapes. The spheres have very similar sizes, with diameters ranging from 10 to 70 nm and wall thicknesses of 3–6 nm. Even larger spherical objects, with mean diameters between 500 nm and 1.2 μm (Fig. 1), were formed upon sonicating a dispersion of a fulleropyrrolidine, in which an ethylammonium group is linked to the pyrrolidine's nitrogen.[58] In other words, placing the positive charge at a larger distance relative to the hydrophobic C_{60} core increases the size of the spheres.

An azafullerene, $(C_{59}N)_2$, and its ultrasonication in acetone also led to a spherical morphology.[59] SEM and TEM confirm that the majority of the sample is in the form of essentially perfect spherical particles that are hollow. They tend to cluster together into quasi-linear assemblies through interconnecting surfaces. As a general feature, the sizes of these azafullerene clusters vary dramatically between 1 and 10 μm.

Finally, intermediately sized spheres were found, when a fulleropyrrolidine ammonium chloride solution of chlorobenzene methanol (10 : 1 *v*/*v*) was left at room temperature for a few days and then dried *in vacuo*.[60] But no sonication was applied to these samples. TEM images reveal diameters that are in the range of 80–130 nm, while complementary AFM led to smaller sizes, 75–95 nm.

In summary, the size of all these spheres falls within a wide range, which can typically reach from 17 nm to 10 μm. It is therefore clear that the size of the spheres is determined by (*i*) the different methods of preparation (*i.e.*, time and type of sonication, presence of co-solvents, deposition, *etc.*), (*ii*) the hydrophobic area left on the fullerene core (*i.e.*, number and nature of the functional groups) and (*iii*) on the side chain appendage of the fullerene spheroid (*i.e.*, balance between attractive and repulsive forces).

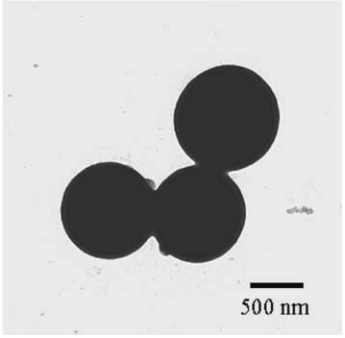

Fig. 1 TEM images of the spheres formed by a fulleropyrrolidine carrying an ethylammonium group.

Crown ether complexation motifs

Crown ethers are very simple macrocyclic ligands constituted of a cyclic array of ether oxygen atoms connected through carbon atoms which have been successfully used as appealing hosts in supramolecular chemistry for cations as well as neutral molecules.

Molecular recognition principles, in the form of crown ether complexation,[62] are the inception for realizing molecularly-organized thin film assemblies and nanoarchitectures. Most prominently, self-assembled monolayers (SAM) were successfully employed to induce the organization of a C_{60} derivative — bearing a crown ether functionality — and an ammonium-terminated alkanethiolate that was attached irreversibly to a gold electrode (Scheme 12).[10] The determination of the surface coverage, as derived on the basis of Osteryoung Square Wave Voltammetry experiments, yielded a value (1.4×10^{-10} mol cm^{-2}), which is well in accord with a fcc closed-packed packing of C_{60} ($\sim 1.9 \times 10^{-10}$ mol cm^{-2}). Complementary desorption experiments confirmed quantitatively the reversibility of this organization principle. In other words, there is no covalent and irreversible linkage of the fullerene moiety to the modified surface. This again substantiated the presence of selective interactions between the crown ether functionality and the ammonium terminal group.

Besides exploiting SAM constructs, the potentiality of a series of fullerene–crown ether conjugates as molecular probes have been examined in complexation assays with potassium, sodium, caesium and lithium cations.[63a] The intriguing objective was to develop a molecular host that would register the complexation event through mutual electronic interactions. Significant perturbations of fullerene's electronic structure were, however, only seen when the bound cation was brought into a position close and tight relative to the C_{60} surface. These requirements were clearly guaranteed in the *trans-1*-bisadduct and, to a somewhat lesser extent, in a *trans-2*- and *trans-3*-bisadduct. Placing the crown ether conjugate, on the other hand, at greater distance from the C_{60} surface eliminated the cation-mediated effects.

In related work, the crown ether conjugate was linked to photoactive C_{60}–TTF donor–acceptor dyads.[63b] Due to their peculiar location — upon complexation of potassium, sodium and lithium — electronic effects were only exerted onto the TTF features. In summary, C_{60} with its highly delocalized

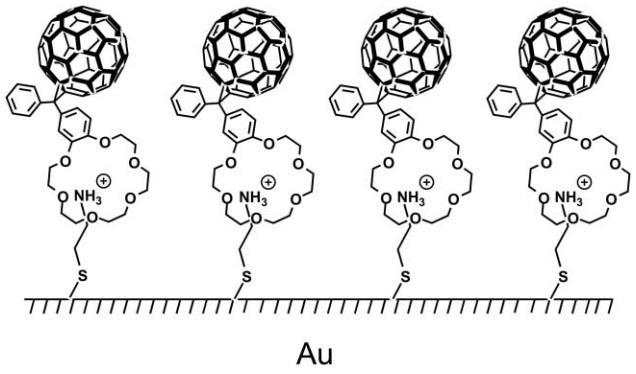

Scheme 12 A self-assembled fullerene–crown ether conjugate monolayer.

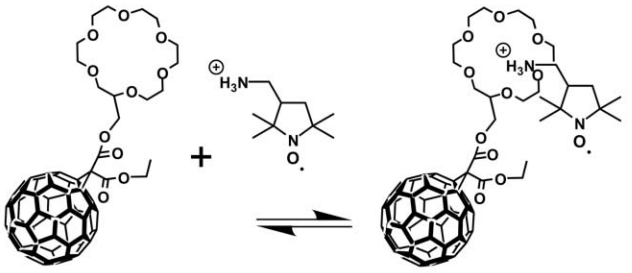

Scheme 13 Formation of a 1 : 1 complex between a fullerene–crown ether conjugate and 3-aminomethyl(2,2,5,5-tetramethylpyrrolindin-1-oxyl).

π-system is not very perceptive for electronically induced changes, unless the electroactive probe is placed in close proximity to ensure strong coupling. Illustrations are found in the following donor–acceptor dyads: Fc–$C_{59}N$, π-stack ZnP–C_{60}, π-stack H_2P–C_{60}, ZnPC–C_{60} and H_2PC–C_{60} (ZnPc and H_2PC stand for zinc phthalocyanine and metal free phthalocyanine, respectively).[64] Common to all these ensembles is the strong coupling between electron donor and electron acceptor as the only probate promoter for perturbating the fullerene's π-system.

In solution, a fullerene–crown ether conjugate, resembling the basic structure of that used for building SAMs, associates in form of a 1 : 1 complex with 3-aminomethyl(2,2,5,5-tetramethylpyrrolindin-1-oxyl).[65] A representation is given in Scheme 13. Upon photoexcitation with visible light, which directs the incident light mainly to the fullerene core, a radical–triplet pair in the quartet excited state has been recorded. Implicit in this picture are strong electronic interactions between the triplet excitations — populated upon irradiation of the associated complex — and an ammonium aminoxyl free radical. Prior to this fundamental work detection of a radical–triplet pair in the quartet excited state was limited to molecular systems, where the radical and triplet precursor were covalently linked, coordinated or linked to a molecular template.

A supramolecular ZnPc–C_{60} dyad (Scheme 14) has been assembled by threading a dibenzylammonium unit attached to a fullerene, through the crown ether of an unsymmetrically substituted phthalocyanine, which contains a dibenzo-24-crown-8.[66] These two components, which both contain different electroactive subunits, can be assembled in a $CHCl_3$ or CH_2Cl_2 solution by threading of the dibenzylammonium chain through the dibenzo-24-crown-8 ring, thus forming the typical stable pseudorotaxane-like complex. The ^{1}H-NMR spectrum of a 1 : 1 mixture in $CDCl_3$ displays the characteristic high field shift and splitting of the resonances assigned to the 1,2-dioxybenzene unit. Diagnostic signals for both free and complexed subunits on the fullerene component were identified and allowed the determination of the association constant ($K_a = 1.53 \times 10^4\ M^{-1}$).

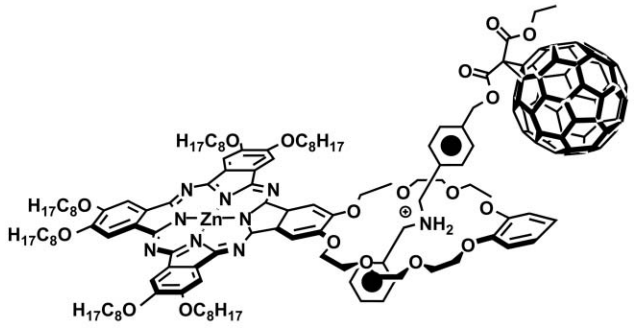

Scheme 14 A supramolecular ZnPc–C_{60} dyad; threading of a dibenzylammonium unit attached to a fullerene through a crown ether of an unsymmetrically substituted phthalocyanine.

Metal mediated motifs

The use of metal ions as synthetic templates has been widely used in supramolecular chemistry as an excellent method to bring about the organization of a number of reacting components in order to control the geometry of the product. Since some metal ions, such as the transition metals, usually present preferred coordination geometries, changes in metal ion may have a strong effect on the nature of the templated product. In the following we will show some of the most remarkable metal mediated supramolecular structures involving fullerenes.

Polypyridyl precursors

The use of copper(I) mediated binding of two separate bidentate 6,6′-disubstituted 2,2′-bipyridine ligands, which are attached to an *o*-quionodimethane derivative of C_{60}, was shown to afford a novel dimeric form of C_{60}, separated by an intervening $[Cu(bpy)_2]^+$ unit.[67a] Up to now, however, only electrochemical investigations were performed with C_{60}-$[Cu(bpy)_2]^+$–C_{60}, which were further complemented by *in-situ* ESR-voltammetric experiments. On account of the efficient and selective formation of copper(II) terpyridines, the corresponding C_{60}–2,2′:6′,2″-terpyridine ligands were also synthesized, which can be viewed as a promising building block for supramolecular chemistry and nanoscience.[67b]

More elaborate is the threading of a C_{60}–rotaxane system (Scheme 15), which relies on the copper(I) templated approach, bearing two C_{60}'s as end-terminating stoppers.[68] In particular, a three component precursor ensemble — a coordinating ring, a redox-active copper(I) center and a bisfunctionalized fragment threaded inside the ring — is reacted with a C_{60}-derivative. Both excited states, the MLCT state of $[Cu(phen)_2]^+$ and the singlet excited state of C_{60}, are substantially quenched. The outcome of these rapid intramolecular deactivation routes is, compared to the excited state energies very different in character and product. For example, deactivation of the fullerene excited state follows an energy transfer mechanism to the adjacent $[Cu(phen)_2]^+$. The latter excited state is mainly quenched by electron transfer to form the charge-separated radical pair comprising an oxidized metal center, namely, $[Cu(phen)_2]^{2+}$ and the one-electron reduced fullerene π-radical anion, $C_{60}^{\bullet -}$.

In parallel work, the design of bis(phenanthroline) complexes, carrying C_{60}-based dendrimers of different complexity, was pursued.[69] Particularly, the successful assembly of 1st, 2nd,

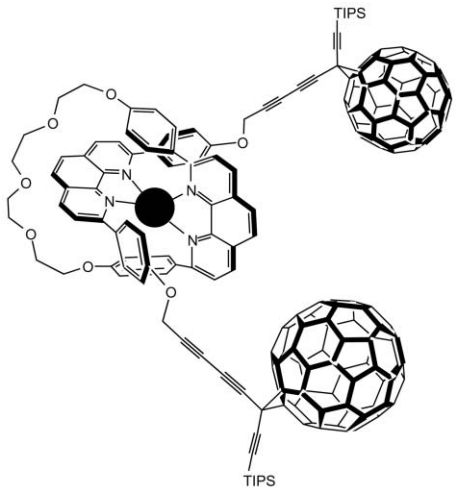

Scheme 15 A C_{60}–rotaxane system.

3rd generations led to dendrimeric peripheries with four, eight and sixteen C_{60} moieties, all surrounding a bis(phenanthroline) copper(I) core, $[Cu(phen)_2]^+$. In the 3rd generation-based ensemble, the 16 C_{60} moieties create a black box around the copper(I) complex, shielding it electronically from the environment. For example, incident light, especially that in the ultraviolet region, fails to penetrate through the densely packed C_{60}-periphery, and does not reach the copper(I) core. Similarly, the indirect route, that is, transduction of singlet or triplet excited state energy from the C_{60}-periphery to the core is unsuccessful. This funnel effect is unlikely to happen, since the excited states of fullerenes are in general very low, with energies typically around 1.75 eV and 1.5 eV for the singlet and triplet manifold, respectively. Thus, an exothermic energy transfer to the copper(I) MLCT excited state (1.85 eV) is energetically unrealizable.

More successful — in terms of photoactivity — is the ruthenium(II) mediated organization of C_{60}–bipyridyl (*i.e.*, electron acceptor) and phenothiazine-bipyridyl (*i.e.,* sacrificial electron donor) building blocks.[70] Importantly, the correspondingly formed ruthenium(II) complex, $[Ru(bpy)_3]^{2+}$, constitutes an important and widely used redox-active chromophore. To document this, the high molar absorptivity of $[Ru(bpy)_3]^{2+}$ should be considered,[71] whose MLCT transitions at 460 nm have extinction coefficients on the order of $\sim 10\,000\ M^{-1}\ cm^{-1}$ relative to $\sim 3\,000\ M^{-1}\ cm^{-1}$ and $\sim 7\,000\ M^{-1}\ cm^{-1}$ for the MLCT transitions in $[Cu(bpy)_2]^+$ and $[Cu(phen)_2]^+$ complexes,[67–69] respectively. Thus, under ambient conditions, the photo- and electro-active C_{60}–$[Ru(bpy)_3]^{2+}$–PTZ triad ensemble, as displayed in Scheme 16, is readily built. As far as the reactivity of C_{60}–$[Ru(bpy)_3]^{2+}$–PTZ is concerned, photoexcitation of the ruthenium(II) chromophore leads to ^{3}*MLCT$[Ru(bpy)_3]^{2+}$, from which a sequence of short-range intramolecular electron and charge transfer reactions evolve. In the final instance, a long-lived charge-separated state, $C_{60}^{\bullet -}$–$[Ru(bpy)_3]^{2+}$–$PTZ^{\bullet +}$, is formed, which in deoxygenated dichloromethane exhibits a lifetime of 1290 ns, before deactivating back to the initial ground state.

Conceptionally, a lot simpler is the organization of C_{60}–$[Ru(bpy)_3]^{2+}$ dyads by a reaction of suitable C_{60}–bipyridyl precursors, bipyridyl ligands (*i.e.*, in a 1:2 stoichiometry) and ruthenium(II) chloride.[72] Different spacers — androstane, polyglycol, crown ester and hexapeptide — were employed as large molecular rulers to separate a C_{60} acceptor unit from the bipyridyl ligand, yielding innovative donor–acceptor ensembles with diverse topographies.[72a,c,e–g] A common feature of all these C_{60}–$[Ru(bpy)_3]^{2+}$ systems is that upon photoexcitation a

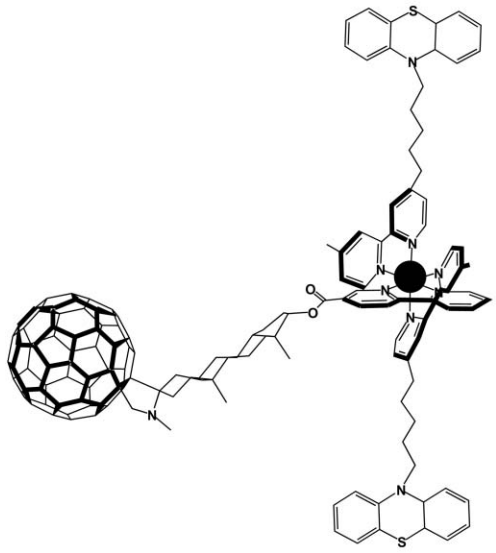

Scheme 16 A C_{60}–$[Ru(bpy)_3]^{2+}$–PTZ triad.

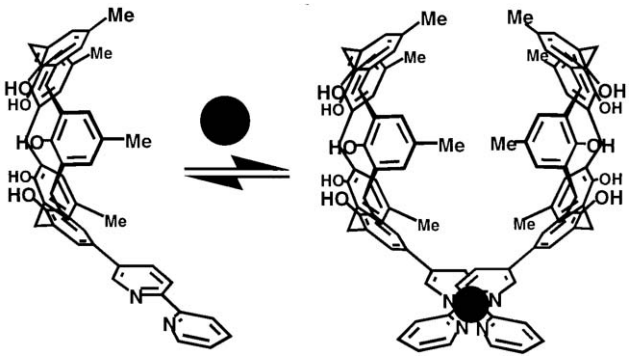

Scheme 17 Metal (silver(I)) mediated organization of a C_{60} receptor.

long-lived charge-separated state, $C_{60}^{\bullet -}$–$[Ru(bpy)_3]^{3+}$ evolves from an intramolecular electron transfer quenching of the ^{3}*(MLCT) state. Owing to the diverse topologies of these dyads, the lifetimes of the $C_{60}^{\bullet -}$–$[Ru(bpy)_3]^{3+}$ turned out to be quite different. For example, in dichloromethane solutions the rigidly spaced C_{60}–*androstane*–$[Ru(bpy)_3]^{2+}$ and C_{60}–*hexapeptide*–$[Ru(bpy)_3]^{2+}$ dyads yield lifetimes of 304 ns and 608 ns, respectively, while no appreciable lifetime was noted for the flexibly spaced C_{60}–*polyglycol*–$[Ru(bpy)_3]^{2+}$ analogue.[73]

Scheme 17 illustrates the metal-mediated organization of another intriguing fullerene receptor.[74] In particular, silver(I) complexation holds together two calix[5]arene precursor units ($K_a = 5.7 \times 10^3\ M^{-1}$) — each carrying a bipyridine ligand — and creates a cavity sufficiently large to bind C_{60} and C_{70}.

Porphyrin precursors

To function efficiently, the donor–acceptor complex by necessity must be weak enough to enable reversible association but strong enough to be selective for a given substrate (*i.e.*, zinc tetraphenylporphyrin — ZnP). The first promising success was presented in the form of a ZnP–*pyridine*–C_{60} complex, in which the reversible coordination of a pyridine functionalized fullerene ligand (*pyridine*–C_{60}) to the square-planar zinc center constitutes a labile but measurable ($K_a \sim 5 \times 10^3\ M^{-1}$) binding motif — Scheme 18.[75] Triggered by light, charge-separation occurs from the excited donor. The weak binding, that governs the equilibrium between dissociation and

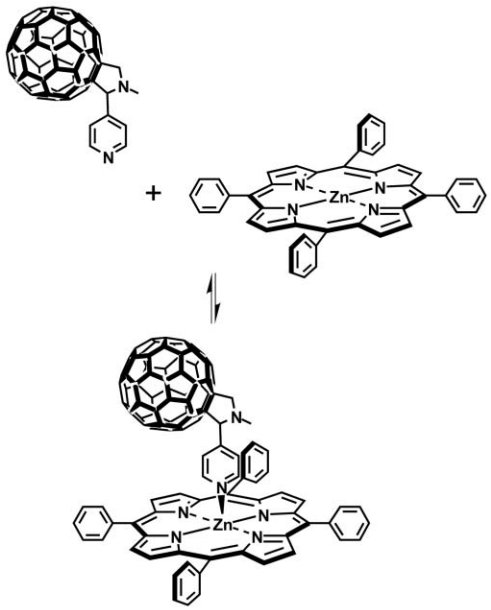

Scheme 18 Reversible coordination of a pyridine functionalized fullerene ligand (*pyridine*–C_{60}) to the square-planar zinc center (ZnP) forming ZnP–*pyridine*–C_{60}.

association of the "metal–pyridine" bond, facilitates then the crucial break-up of $ZnP^{\bullet+}$–*pyridine*–$C_{60}^{\bullet-}$. In ZnP–*pyridine*–C_{60}, the free radical ions — $ZnP^{\bullet+}/C_{60}^{\bullet-}$ — live for tens of microseconds and charge-recombination is limited to an intermolecular diffusion.

Complexation of *pyridine*–C_{60} to a ruthenium tetraphenylporphyrin (RuP), on the other hand, forms the quite stable RuP–*pyridine*–C_{60} complex.[75d] The π-back-bonding strengthens the "metal–pyridine" bond relative to the ZnP–*pyridine*–C_{60} analog, in which the bonding has a weak σ-character. As a consequence, the intramolecular charge-separated $RuP^{\bullet+}$–*pyridine*–$C_{60}^{\bullet-}$ recombines rapidly on the picosecond time scale (< 4000 ps), since the diffusional splitting of the radical pair is hindered by the stable "metal–pyridine" bond.

As far as the solid state structure of ZnP–*pyridine*–C_{60} is concerned, its X-ray structure supports several key features.[75e] Firstly, and, most importantly, the tilting of the C_{60} unit towards the porphyrin is clearly discernable. Secondly, the edge-to-edge distance, that is, the closest distance between the porphyrin π-ring carbon and the C_{60} carbon of the axially linked fulleropyrrolidine is 3.51 Å. Thirdly, the zinc to axially coordinated pyridyl nitrogen distance is 2.158 Å. Finally, the center-to-center distance between the porphyrin zinc ion and C_{60} is ~9.53 Å.

Following principally the same motif, a more linearly aligned supramolecular architecture was assembled, based on linking a heterofullerene acceptor (*pyridine*–$C_{59}N$) to the central zinc atom of a zinc tetra(*p-tert*-butylphenyl)porphyrin (ZnP) donor.[76] The linear refinement was achieved by attaching the donor pyridine ring to the $C_{59}N$ moiety, yielding *pyridine*–$C_{59}N$, by the Mannich functionalization method of the dimer, $(C_{59}N)_2$. The ZnP–*pyridine*–$C_{59}N$ adduct is also ideally suited for devising integrated model systems to transmit and process solar energy. Depending on the solvent either photoinduced singlet–singlet energy transfer or electron-transfer was observed. The latter process takes place in *o*-dichlorobenzene as solvent and leads to the corresponding *pyridine*–$C_{59}N$ π-radical anion and ZnP π-radical cation.

A fascinating modification of the ZnP–*pyridine* coordination focuses on the modulation of the donor–acceptor proximity by controlling a "tail-on"/"tail-off" binding mechanism.[77] In this work, the *pyridine*–C_{60} ligand is covalently attached to the phenyl group of ZnP and the nitrogen of the pyrrolidine through a flexible chain (Scheme 19). The defined spatial

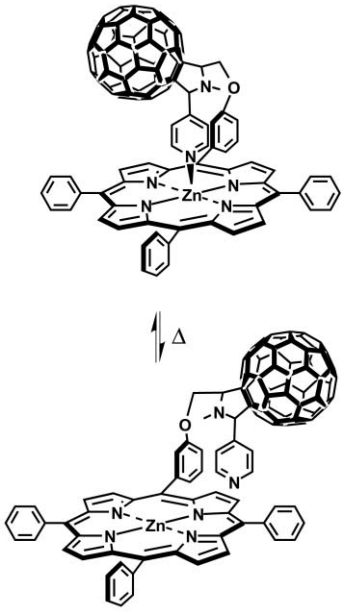

Scheme 19 Temperature dependent equilibrium between "tail-on"/"tail-off".

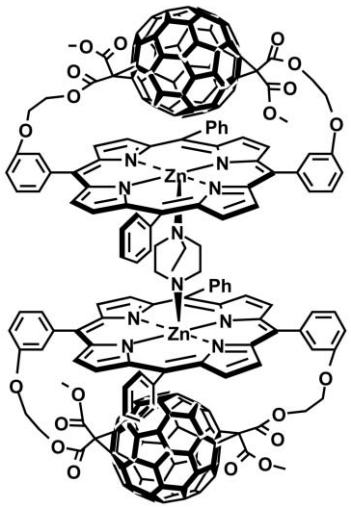

Scheme 20 A linear C_{60}–ZnP–DABCO–ZnP–C_{60} stack.

organization is controlled *via* temperature variation or replacement of the axial ligand with 3-picoline. As far as charge-separation rates and efficiencies are concerned in the "tail-off" status (*i.e.,* ZnP/*pyridine*–C_{60}) both parameters are slightly changed in comparison with the results of the "tail-on" status (*i.e.*, ZnP–*pyridine*–C_{60}), suggesting through-space interactions in the earlier. In line with this assumption falls the observation that also an acceleration of the charge-recombination comes to light in the "tail-off" form.

Ultimately, the objective is to devise linear architectures of higher complexity, that is, triads, tetrads and pentads. This was accomplished *via* the titration of *trans-2*-ZnP–C_{60} with diazabicyclooctane (DABCO) in non-coordinating media to avoid competition in the complexation process.[78] The bidentate DABCO ligand exhibits a number of noteworthy features, (*i*) it forms square pyramidal 1 : 1- or 2 : 1-complexes with ZnP in non-coordinating solvents and (*ii*) it is also a good electron donor. An explication is given in Scheme 20. Importantly, charge-recombination kinetics in the primary building block (*i.e., trans-2*-ZnP–C_{60}), which are deeply in the Marcus inverted region, indicate that the large $-\Delta G_{CR}^{\circ}$ values in non-polar toluene are advantageous in stabilizing the $ZnP^{\bullet+}$–$C_{60}^{\bullet-}$ radical pair. Depending on the relative concentrations, namely, that of DABCO and *trans-2*-ZnP–C_{60}, the precursor ZnP–C_{60} dyad was transformed *step-by-step* into DABCO–ZnP–C_{60} (*i.e.*, micromolar concentrations) and C_{60}–ZnP–DABCO–ZnP–C_{60} (*i.e.*, millimolar concentrations). In these newly formed ensembles, the lifetimes of the charge-separated states vary markedly with the ensemble constitution. For example, a significant improvement is seen upon going from *trans-2*-$ZnP^{\bullet+}$–$C_{60}^{\bullet-}$ (toluene: τ = 619 ps) and $DABCO^{\bullet+}$–ZnP–$C_{60}^{\bullet-}$ (toluene: τ = 1980 ps) to C_{60}–ZnP–$DABCO^{\bullet+}$–ZnP–$C_{60}^{\bullet-}$ (toluene: τ = 2280 ps). In summary, the simple addition of extra components, which self-assemble to the precursor in a controlled manner, is an effective mode to gain control over the charge-recombination rates.

In a different example, regulating the donor–acceptor separations and orientations was completed by self-assembling a flexible ZnP–C_{60}–ZnP system with DABCO, affording rigid, confined model ensembles.[79] The photophysics of the precursor systems — *meta*-ZnP–C_{60}–ZnP and the more electron-rich *para*-ZnP–C_{60}–ZnP – are governed by a photoinduced electron transfer evolving from the ZnP singlet excited state to the electron accepting fullerene. The resulting $ZnP^{\bullet+}$–$C_{60}^{\bullet-}$–ZnP states decayed on a time scale of a few hundred nanoseconds to regenerate the ground state. For example, in *o*-dichlorobenzene the actual values are 150 ns and 290 ns in the *meta*-ZnP–C_{60}–ZnP and *para*-ZnP–C_{60}–ZnP isomers, respectively. A threefold

reactivation of the ^{1}*ZnP fluorescence was seen upon addition of DABCO to toluene or *o*-dichlorobenzene solutions of *meta*-ZnP–C_{60}–ZnP or *para*-ZnP–C_{60}–ZnP, which also led to a slow-down of the decay and grow-in kinetics of ^{1}*ZnP and $ZnP^{\bullet+}$–$C_{60}^{\bullet-}$ features, respectively. As a result of the successful complexation of DABCO to the vacant sites of the two ZnP (*i.e.*, dz^2-orbitals) the donor–acceptor separation is expanded considerably. In polar *o*-dichlorobenzene these stable ensembles are subject to a rapid intramolecular electron transfer to yield long-lived radical pairs with lifetimes close to a microsecond ($\sim$700 ns). This unmistakably confirms that the simple addition of a suitable component leads to a nearly five-fold improvement of the radical pair stability, besides an overall higher quantum yield of formation (Φ). Conversely, in non-polar toluene energy transfer replaces electron transfer in deactivating the photoexcited chromophore, ^{1}*ZnP, forming, in the final instance, the fullerene triplet excited state.

Linear arrays are built when larger DABCO-millimolar-concentrations are added to ZnP–C_{60}–ZnP. First, at these high concentrations precipitation of a poorly soluble oligomeric material is observed, which can be re-suspended in *o*-dichlorobenzene. It is interesting to note that the lifetime of the radical pair in these linear structures gives rise to a further improvement (7.5 μs): a sufficiently fast separation of charges along the longitudinal axis is probably responsible for this consequence.

Summarizing, these metal-mediated concept, namely, coordination of a fullerene–pyridine ligand or DABCO by a macrocyclic π-system are very general and were extended successfully to zinc complexes of phthalocyanines, porphycenes and corrphycene macrocycles.[75] Interestingly, the binding strength reveals a close resemblance with the oxidation potential of the macrocyclic π-system: porphycene > porphyrin.

Electrostatic motifs

The huge amount of fullerene derivatives synthesized in recent years has resulted in the preparation of modified fullerenes and fullerene ensembles which are clearly located in the field of supramolecular chemistry and, particularly, within the so-called electrostatic binding interactions with a different range of attractive and repulsive forces.

DNA-based assemblies

The first systematic exploration of electrostatic interaction as a probate means to bind C_{60} — with cationic headgroups — to a suitable template was reported in binding assays with duplex DNA.[80] In particular, a *N,N*-dimethylfulleropyrrolidinium salt and three isomeric fulleropyrrolidines carrying pyridinium moieties all bind to double stranded DNA with diverse affinities. Contributions from electrostatic and also hydrophobic interactions with the phosphate groups along the DNA backbone and the DNA grooves, respectively, control the binding modes. As far as the action of light is concerned, all derivatives cleaved double stranded DNA under photoirradiation promoted through singlet oxygen. The latter species evolves as a product of the reaction of triplet excited C_{60} with molecular oxygen. Importantly, preferential binding to the DNA grooves brings the C_{60} photosensitizer closer to the nucleic bases and enhances the cleavage efficiency.

More recently, a ''two-handed'' C_{60} derivative — carrying two protonated diamine side chains — binds *via* an electrostatic interaction to duplex DNA.[81] In addition it condenses and allows the complexed DNA to be delivered into and transiently expressed in the target cell. Despite of the intrinsic photoactivity of C_{60}, no differences were noted when the transfection assays were carried out under ambient light or black light.

Nanonetworks on indium–tin-oxide (ITO) electrodes

The scope of a different work is to devise electrostatically built nanonetworks that will lead to significant improvements in energy conversion and transport.[82,83] In particular, the successful construction of photoactive ITO-electrodes was accomplished based on a *layer-by-layer* (LBL) approach (Scheme 21). The strategy, employing donor-linked fullerenes bearing positively charged functionalities, provides several advantages: Firstly, and by far the most important, it allows control over the thickness and composition of the assembled films at the molecular level. Secondly, it guarantees the specific alignment and the orientation of the incorporated donor–acceptor system as a crucial means to facilitate the electron transfer between adjacent layers. Thirdly, repulsion of equally charged substrates restricts each assembly procedure to single layer coverage.

To visualize the electrostatically driven deposition of poly(styrene-4-sulfonate) (PSS) and C_{60}-based materials, as they were assembled on poly(diallydimethylammonium) chloride (PDDA) the correspondingly modified ITO electrodes were imaged by AFM. The morphology of PDDA/PSS/C_{60}-based material coatings as observed by AFM is significantly different from those of PDDA and PDDA/PSS. The surface becomes uniformly covered with characteristic 2D aggregates, which assemble in a continuous uniform film. By the repetition of the deposition sequence, that is the coverage with a layer of PSS and a layer of fullerene, the LBL stacking of sandwiched composites was accomplished.

From these results and complementary ellipsometric measurements it was inferred that the C_{60}-based materials organize

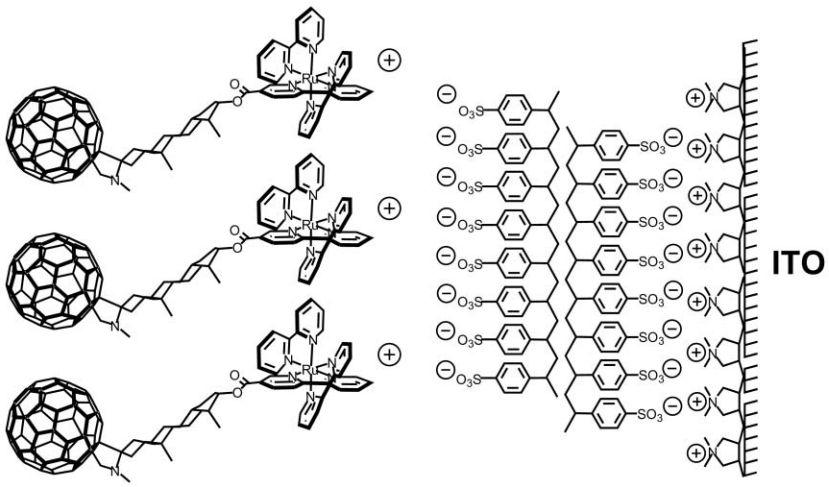

Scheme 21 Layer-by-layer (LBL) approach for the construction of photoactive ITO-electrodes.

onto PSS in an electrostatically directed manner, guaranteeing the satisfactory and uniform stacking of individually deposited LBL films. This involves, for example, assembly of the positively-charged ruthenium(II)–polypyridyl complex onto PSS, while for the fulleropyrrolidinium salts just the pyrrolidinium group is responsible for the anchoring onto the PSS template. In all cases, the monolayer coverage creates a predominantly hydrophobic surface, constituted by 2D domains of C_{60} cores. Strong π–π associations, as they prevail generally between individual fullerene molecules, are then the driving force for the 1D controlled build-up of another monolayer on this hydrophobic surface.

Special attention should be directed to an approach, which aims at controlling the morphology of nanostructured films.[82b] In this work, a ferrocene moiety was probed as the electron donor, connected to a *N,N*-dimethylfulleropyrrolidinium salt through a rigid androstane spacer, C_{60}–*androstane*–Fc. A surprisingly high level of intermolecular organization of C_{60}–*androstane*–Fc was found, when assembled in the LBL films. While the images taken of PDDA and PDDA/PSS reveal fairly flat surfaces, after adsorption of the dyad, rod-like superstructures of 1–3 microns in length appear (Fig. 2). At the same time, the similarly prepared films from C_{60}–*oligoethylene*–Fc, connected by a flexible oligoethylene bridge, did not reveal any intralayer self-organization. Therefore, the rigidity of C_{60}–*androstane*–Fc leads to their self-assembly in rows due to strong van der Waals attraction between them.

The photoaction spectra of assembled layers of the *N,N*-dimethylfulleropyrrolidinium–ferrocene dyad on ITO track the absorption spectrum of the *N,N*-dimethylfulleropyrrolidinium moiety with a maximum around 375 nm, thereby indicating that the incorporated dyad retains its basic reactivity as a photosensitizer. The photocurrent of monolayer coverage under deoxygenated conditions reveals a three- and ninety-fold enhancement relative to the earlier investigated fulleropyrrolidinium salt, and C_{60}–*oligoethylene*–Fc, respectively. This performance improvement can be attributed to the charge conductance along the fullerene nanowires and, thus, facilitating the charge diffusion from the photoactive centers to the electrodes, due to extensive interpenetration of the layers leading to multiple contacts between the fullerene nanowires. Importantly, in oxygenated systems, an additional increase in the photocurrent is seen. This increase is related to the favored electron transfer from the photolytically generated fullerene π-radical anion to molecular oxygen. $O_2^{\bullet -}$ acts then as an electron carrier transferring the charges to the electrode.

A similar strategy has been practised in the construction of photoactive ITO electrodes *via* the electrostatic assembly of fullerol, polyhydroxylated $C_{60}(OH)_x$, in conjunction with PDDA, yielding ultrathin multilayer films.[84] In particular, highly uniform, transparent, micrometer-thick $C_{60}(OH)_x$ films were fabricated and characterized by absorption spectroscopy, ellipsometry and AFM. Following this more general work, the preparation and characterization of rectifying photovoltaic heterostructure devices, made of poly(phenylenevinylene) (PPV) and C_{60}, was pursued. In these samples the structures are bilayer-blocks made of PPV/poly(acrylic acid) (PAA) and C_{60}/poly(allylamine hydrochloride) (PAAH), which serve as electron donor and electron acceptor, respectively. The heterojunctions were built from solution *via* electrostatic interactions: The electron donor was made of individually adsorbed monolayers of a charged, nonconjugated form of PPV and PAA, while alternating monolayers of sulfonated C_{60} and PAAH were fabricated for the electron acceptor. Low dark currents and high open circuit voltages characterize the heterojunctions, whose mode of action is based on a photoinduced electron transfer between PPV and C_{60}.

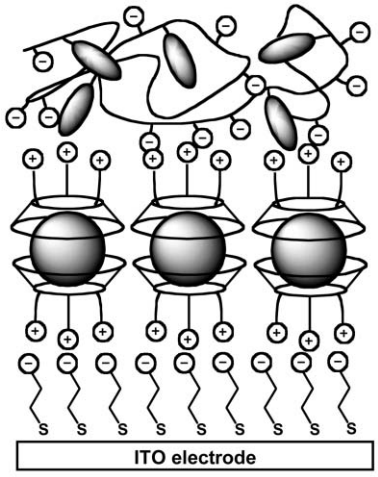

Scheme 22 Schematic illustration of an electrostatically-driven assembly of a cationic C_{60}–(homoocacalix[3]arene) inclusion complex and an anionic porphyrin polymer.

Finally, a study should be mentioned that combines two of the above-discussed motifs, that is, electrostatic and π-stack motifs: electrostatically-driven assembly of a cationic C_{60}–(homooxacalix[3]arene) inclusion complex and an anionic porphyrin polymer (Scheme 22).[85] The photocurrent flow, along the porphyrin–C_{60}–ITO gradient, gives rise to quantum yield of 21%, which is comparable to the 25% found for a molecular triad (*i.e.*, C_{60}–porphyrin–ferrocene) assembled onto a gold electrode.

In short, electrostatic assembly has emerged as a viable and promising means to construct molecular devices such as photoactive ITO electrodes, which are employable for solar energy conversion. It was shown that the characteristics of the photoelectrochemical cell performance depend significantly upon the architecture of the nanostructured film and on what is assembled in conjunction with C_{60} as the acceptor material.

Template motifs

Creation of complex networks from very simple components, that is, an ionic component (*i.e.*, silver(I) nitrate) and C_{60}, is

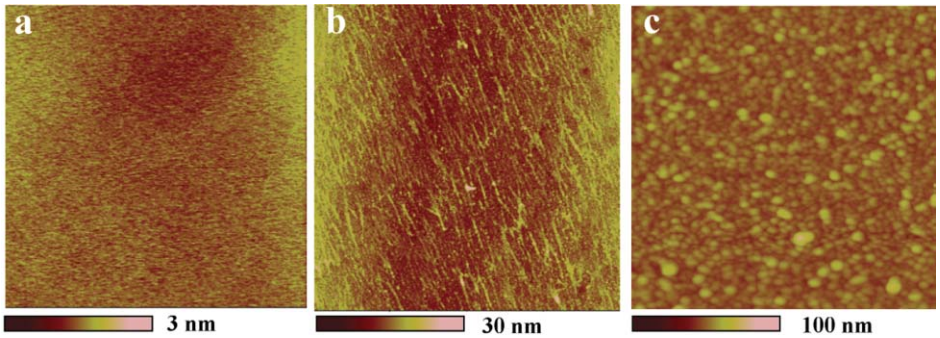

Fig. 2 AFM topography images (1 μm × 1 μm) of (a) PDDA/PSS), (b) PDDA/PSS/C_{60}–*androstane*–Fc and (c) of PDDA/PSS/C_{60}–*oligoethylene*–Fc.

reported, which are stable in the presence of air and moisture.[86] The silver nitrate portion forms a zeolite network shaping rounded cavities that are occupied by C_{60} moieties. Importantly, the silver network encapsulates each C_{60} in a fashion that precludes any movement. Since the silver–carbon distance (2.213 Å) is quite short and the location of the silver ion is directly over a single carbon atom, η^1-coordination is involved in the cocrystallization process.

The genome of the human immunodeficiency virus (HIV) is packaged within an unusual conical core particle located-at the center of the infectious virion.[87] The active site of this enzyme is lined almost exclusively by hydrophobic amino acids, with the exception of two catalytic aspartic acids. C_{60}, on the other hand, is a template, complementary in many aspects to the active site. In fact, it was demonstrated that competitive inhibition precludes inhibitor binding, while C_{60} — functioning as a substrate — is bound. As the main driving force behind this template organization cooperative effects stemming from non-polar van der Waals and electrostatic interactions are assumed. Obviously, the hydrophobicity of the non-polar active site surface and that of the C_{60} surface are well balanced. In addition, salt bridges between the catalytic aspartates of the active site and a cationic site on the C_{60} surface led to an increased binding affinity.

Summary and outlook

This article has demonstrated the effectiveness of employing fullerenes in biomimetic strategies for devising thermodynamic stable but kinetic labile 1D, 2D, or 3D networks. These strategies (highly directional hydrogen bondings; π-stack motifs including concave–convex, planar–convex and convex–convex interactions; crown ether complexation; metal mediated and electrostatic interactions) provide the means for an evident trend towards the facile preparation of precise structures never before accomplished by conventional synthetic chemistry. The most important aspect in this area is the regulation of the inherently weak forces seen in biomimetic organization principles on a molecular basis. In this context, the current concepts illustrate that relating size and shape to the function of the resulting composites led to composites with new and original properties. Unquestionably, the peculiar shape and unique electronic properties of fullerenes — as stiff molecular scaffolds — have an important bearing on the design of novel, well-ordered supramolecular arrays.

Despite some remarkable recent successes, it is clear that the examples discussed in this Feature Article represent only the tip of the iceberg. More research in this relatively new area is needed to fully explore the possibilities offered by these materials, for example, in the production of active as well as passive devices. This underlines more than ever the great need for creative synthetic chemistry, which will ensure that eventually fullerenes may become an important building block of future technologies, such as optoelectronics, batteries and photovoltaics.

Acknowledgement

This work was supported by the Office of Basic Energy Sciences of the Department of Energy and the DGESIC of Spain (Project PB98-0818). This is document NDRL-4381 from the Notre Dame Radiation Laboratory.

References

1 (*a*) G. McDermott, S. M. Priece, A. A. Freer, A. M. Hawthornthwaite-Lawless, M. Z. Papiz, R. J. Cogdell and N. W. Isaaacs, *Nature*, 1995, **374**, 517–521; (*b*) J. Barber, *Nature*, 1988, **333**, 114–114; (*c*) V. Balzani and L. de Cola, Eds. *Supramolecular Chemistry*, NATO ASI Series, Kluwer Academic Publishers, Dordrech, 1992.
2 *The Photosynthetic Reaction Center*, ed. J. Deisenhofer and J. R. Norris, Academic Press, New York, 1993.
3 (*a*) F. Vögtle, *Supramolecular Chemistry*, Wiley, Chichester, 1991; (*b*) J. M. Lehn, *Supramolecular Chemistry- Concepts and Perspectives*, VCH, Weinheim, 1995; (*c*) J. W. Steed and J. L. Atwood, *Supramolecular Chemistry*, Wiley, Chichester, 2000.
4 (*a*) *Comprehensive Supramolecular Chemistry Vol. 1-10*, eds. J. L. Atwood, J. E. D. Davies, D. D. MacNicol, F. Vögtle and J.-M. Lehn, Pergamon/Elsevier, Oxford, UK, 1996; (*b*) L. F. Lindoy and I. M. Atkinson, *Self-Assembly in Supramolecular Systems*, Royal Society of Chemistry, Cambridge, UK, 2000.
5 *Nanoparticles and Nanostructured Films*, ed. J. H. Fendler, Wiley, Weinheim, 1998.
6 (*a*) F. Diederich and R. Kessinger, *Acc. Chem. Res.*, 1999, **32**, 537–545; (*b*) *Fullerenes and Related Structures*, ed. A. Hirsch, *Top. Curr. Chem.*, Vol. 199, Springer, Berlin, 1999; (*c*) M. Prato and M. Maggini, *Acc. Chem. Res.*, 1998, **31**, 519–526; (*d*) *Lecture Notes on Fullerenes Chemistry*; ed. R. Taylor, Imperial College Press, London, 1999.
7 (*a*) D. Philp and J. F. Stoddart, *Angew. Chem., Int. Ed. Engl.*, 1996, **35**, 1155–1196; (*b*) D. S. Lawrence, T. Jiang and M. Levitt, *Chem. Rev.*, 1995, **95**, 2229–2260; (*c*) D. C. Sherrington and K. A. Taskinen, *Chem. Soc. Rev.*, 2001, **30**, 83–93.
8 For a recent review, see C. Schmuck and W. Wienand, *Angew. Chem., Int. Ed.*, 2001, **40**, 4363–4369.
9 For recent reviews on fullerene containing donor–acceptor ensembles and fullerene anions see (*a*) H. Imahori and Y. Sakata, *Adv. Mater.*, 1997, **9**, 537–546; (*b*) M. Prato, *J. Mater. Chem.*, 1997, **7**, 1097–1109; (*c*) N. Martin, L. Sanchez, B. Illescas and I. Perez, *Chem. Rev.*, 1998, **98**, 2527–2547; (*d*) H. Imahori and Y. Sakata, *Eur. J. Org. Chem.*, 1999, 2445–2457; (*e*) F. Diederich and M. Gomez-Lopez, *Chem. Soc. Rev.*, 1999, **28**, 263–277; (*f*) D. M. Guldi, *Chem. Commun.*, 2000, 321–327; (*g*) D. M. Guldi and M. Prato, *Acc. Chem. Res.*, 2000, **33**, 695–703; (*h*) C. A. Reed and R. D. Bolskar, *Chem. Rev.*, 2000, **100**, 1075–1119; (*i*) D. Gust, T. A. Moore and A. L. Moore, *J. Photochem. Photobiol. B*, 2000, **58**, 63–71; (*j*) D. Gust, T. A. Moore and A. L. Moore, *Acc. Chem. Res.*, 2001, **34**, 40–48.
10 F. Arias, L. A. Godinez, S. R. Wilson, A. E. Kaifer and L. Echegoyen, *J. Am. Chem. Soc.*, 1996, **118**, 6086–6087.
11 F. Diederich, L. Echegoyen, M. Gomez-Lopez, R. Kessinger and J. Fraser Stoddart, *J. Chem. Soc., Perkin Trans. 2*, 1999, 1577–1586.
12 J. J. González, S. González, E. M. Priego, C. Luo, D. M. Guldi, J. De Mendoza and N. Martín, *Chem. Commun.*, 2001, 163–164.
13 M. T. Rispens, L. Sánchez, J. Knol and J. C. Hummelen, *Chem. Commun.*, 2001, 161–162.
14 (*a*) R. C. Haddon, L. E. Brus and K. Raghavachari, *Chem. Phys. Lett.*, 1986, **131**, 165–169; (*b*) K. Prassides, H. W. Kroto, R. Taylor, D. R. M. Walton, W. I. F. David, J. Tomkinson, R. C. Haddon, M. J. Rosseinsky and D. W. Murphy, *Carbon*, 1992, **8**, 1277–1286; (*c*) M. K. Kelly, P. Etchegoin, D. Fuchs, W. Krätschmer and K. Fostiropulos, *Phys. Rev. B*, 1992, **46**, 4963–4968; (*d*) R. C. Haddon, *Science*, 1993, **261**, 1545–1550.
15 C. A. Mirkin and W. B. Caldwell, *Tetrehedron*, 1996, **52**, 5113–5130 and references cited therein.
16 (*a*) T. Andersson, K. Nilsson, M. Sundahl, G. Westman and O. Wennerstroem, *Chem. Commun.*, 1992, 604–606; (*b*) M. Sundahl, T. Andersson, K. Nilsson, O. Wennerstroem and G. Westman, *Synth. Met.*, 1993, **55**, 3252–3257; (*c*) T. Andersson, G. Westman, O. Wennerstroem and M. Sundahl, *J. Chem. Soc., Perkin Trans. 2*, 1994, 1097–1101; (*d*) E. Constable, *Angew. Chem., Int. Ed.*, 1994, **33**, 2269–2271; (*e*) K. I. Priyadarsini, H. Mohan, A. K. Tyagi and J. P. Mittal, *J. Phys. Chem.*, 1994, **98**, 4756–4759; (*f*) Z. Yoshida, H. Takekuma, S. Takekuma and Y. Matsubara, *Angew. Chem., Int. Ed.*, 1994, **33**, 1597–1599; (*g*) Y. Kuroda, H. Nozawa and H. Ogoshi, *Chem. Lett.*, 1995, 47–48; (*h*) G. Marconi, B. Mayer, C. T. Klein and G. Koehler, *Chem. Phys. Lett.*, 1996, **260**, 589–594; (*i*) K. Komatsu, K. Fujiwara, Y. Murata and T. Braun, *J. Chem. Soc., Perkin Trans. 1*, 1999, 2963–2966; (*j*) A. Buvari-Barcza, J. Rohonczy, N. Rozlosnik, T. Gilanyi, B. Szabo, G. Lovas, T. Braun, S. Samal and K. E. Geckeler, *Chem. Commun.*, 2000, 1101–1102; (*k*) J. Samu and L. Barcza, *J. Chem. Soc., Perkin Trans. 2*, 2001, 191–196.
17 C. Zonta, S. Cossu and O. DeLucchi, *Eur. J. Org. Chem.*, 2000, 1965–1971.
18 (*a*) R. M. Williams and J. W. Verhoeven, *Recl. Trav. Chim. Pays-Bas*, 1992, **11**, 531–532; (*b*) J. L. Atwood, G. A. Koutsantonis and

C. L. Raston, *Nature*, 1994, **369**, 229–231; (*c*) T. Suzuki, K. Nakashima and S. Shinkai, *Chem. Lett.*, 1994, 699–702; (*d*) N. S. Isaacs, P. J. Nichols, C. L. Raston, C. A. Sandova and D. J. Young, *Chem. Commun.*, 1997, 1839–1840; (*e*) T. Haino, M. Yanase and Y. Fukazawa, *Angew. Chem., Int. Ed.*, 1997, **36**, 259–960; (*f*) J. L. Atwood, L. J. Barbour, C. L. Raston and I. B. N. Sudria, *Angew. Chem. Int. Ed.*, 1998, **37**, 981–983; (*g*) T. Haino, M. Yanase and Y. Fukazawa, *Angew. Chem., Int. Ed.*, 1998, **37**, 997–998; (*h*) K. Tsubaki, K. Tanaka, T. Kinoshita and K. Fuji, *Chem. Commun.*, 1998, 895–896; (*i*) M. Yanase, T. Haino and Y. Fukazawa, *Tetrahedron Lett.*, 1999, **40**, 2781–2784; (*j*) J. L. Atwood, L. J. Barbour, P. J. Nichols, C. L. Raston and C. A. Sandoval, *Chem. Eur. J.*, 1999, **5**, 990–996; (*k*) F. C. Tucci, D. M. Rudkevich and J. Rebek, *J. Org. Chem.*, 1999, **64**, 4555–4559; (*l*) I. Schlachter, U. Hoeweler, W. Iwanek, M. Urbaniak and J. Mattay, *Tetrahedron*, 1999, **55**, 14931–14940; (*m*) S. Bhattacharya, S. K. Nayak, S. Chattopadhyay, M. Banerjee and A. K. Mukherjee, *J. Chem. Soc., Perkin Trans. 2*, 2001, 2292–2297.

19 (*a*) P. E. Georghiou, S. Mizyed and S. Chowdhury, *Tetrahedron Lett.*, 1999, **40**, 611–614; (*b*) S. Mizyed, P. E. Georghiou and M. Ashram, *J. Chem. Soc., Perkin Trans. 2*, 2000, 277–280; (*c*) S. Mizyed, P. R. Tremaine and P. E. Georghiou, *J. Chem. Soc., Perkin Trans. 2*, 2001, 3–6; (*d*) S. Mizyed, M. Ashram, D. O. Miller and P. E. Georghiou, *J. Chem. Soc., Perkin Trans. 2*, 2001, 1916–1919.

20 (*a*) J. W. Steed, P. C. Junk, J. L. Atwood, M. J. Barnes, C. L. Raston and R. S. Burkhalter, *J. Am. Chem. Soc.*, 1994, **116**, 10346–10347; (*b*) M. J. Hardie, P. D. Godfrey and C. L. Raston, *Chem. Eur. J.*, 1999, **5**, 1828–1833.

21 (*a*) D. M. Guldi, H. Hungerbühler, E. Janata and K.-D. Asmus, *J. Chem. Soc., Chem. Commun.*, 1993, 84–85; (*b*) P. Boulas, W. Kutner, M. T. Jones and K. M. Kadish, *J. Phys. Chem.*, 1994, **98**, 1282–1287; (*c*) K. I. Priyadarsini, H. Mohan, J. P. Mittal, D. M. Guldi and K.-D. Asmus, *J. Phys. Chem.*, 1994, **98**, 9565–9569; (*d*) V. Ohlendorf, A. Willnow, H. Hungerbühler, K.-D. Asmus and D. M. Guldi, *J. Chem. Soc., Chem. Commun.*, 1995, 759–760.

22 B. Paci, G. Amoretti, G. Arduini, G. Ruani, S. Shinkai, T. Suzuki, F. Ugozzoli and R. Caciuffo, *Phys. Rev. B*, 1997, **55**, 5566–5569.

23 R. M. Williams, J. M. Zwier, J. W. Verhoeven, G. H. Nachtegaal and A. P. M. Kentgens, *J. Am. Chem. Soc*, 1994, **116**, 6965–6966.

24 A. Ikeda, Y. Suzuki, M. Yoshimura and S. Shinkai, *Tetrahedron*, 1998, **54**, 2497–2508.

25 A. Ikeda, M. Yoshimura and S. Shinkai, *Tetrahedron Lett.*, 1997, **38**, 2107–2110.

26 S. A. Olsen, A. M. Bond, R. G. Compton, G. Lazarev, P. J. Mahon, F. Marken, C. L. Raston, V. Tedesco and R. D. Webster, *J. Phys. Chem. A*, 1998, **102**, 2641–2649.

27 S. D.-M. Islam, M. Fujitsuka, O. Ito, A. Ikeda, T. Hatano and S. Shinkai, *Chem. Lett.*, 2000, 78–79.

28 J. L. Bourdelande, J. Font, R. Gonzalez-Moreno and S. Nonell, *J. Photochem. Photobiol. A*, 1998, **115**, 69–71.

29 D. Sun and C. A. Reed, *Chem. Commun.*, 2000, 2391–2392.

30 (*a*) P. Zhou, Z. H. Dong, A. M. Rao and P. C. Eklund, *Chem. Phys. Lett.*, 1993, **211**, 337–340; (*b*) Y. Wang, J. M. Holden, Z. H. Dong, X. X. Bi and P. C. Eklund, *Chem. Phys. Lett.*, 1993, **211**, 341–345; (*c*) A. M. Rao, P. Zhou, K.-A. Wang, G. T. Hager, J. M. Holden, Y. Wang, W.-T. Lee, X.-X. Bi, P. Ecklund, D. S. Cornett, M. A. Duncan and I. J. Amster, *Science*, 1993, **259**, 955; (*d*) Y. Wang, J. M. Holden, X.-X. Bi and P. C. Eklund, *Chem. Phys. Lett.*, 1994, **217**, 413–417; (*e*) Y. Iwasa, T. Arima, R. M. Fleming, T. Siegrist, O. Zhou, R. C. Haddon, L. J. Rothberg, K. B. Lyons, H. L. Carter, A. F. Hebard, R. Tycko, G. Dabbagh, J. J. Krajewski, G. A. Thomas and T. Yagi, *Science*, 1994, **264**, 1570; (*f*) P. W. Stephens, G. Bortel, G. Faigel, M. Tegze, A. Janossy, S. Pekker, G. Oszlanyi and L. Forro, *Nature.*, 1994, **370**, 636; (*g*) P. C. Eklund, A. M. Rao, P. Zhou, Y. Wang and J. M. Holden, *Thin Solid Films*, 1995, **257**, 185–203.

31 (*a*) O. D. Fox, M. G. B. Drew, E. J. S. Wilkinson and P. D. Beer, *Chem. Commun.*, 2000, 391–392; (*b*) O. D. Fox, M. G. B. Drew and P. D. Beer, *Angew. Chem., Int. Ed.*, 2000, **39**, 136–140.

32 (*a*) H. Hungerbühler, D. M. Guldi and K.-D. Asmus, *J. Am. Chem. Soc.*, 1993, **115**, 3386–3387; (*b*) D. M. Guldi, H. Hungerbühler and K.-D. Asmus, *J. Phys. Chem.*, 1995, **99**, 13487–13493; (*c*) D. M. Guldi, *J. Phys. Chem. A*, 1997, **101**, 3895–3900; (*d*) D. M. Guldi, *J. Phys. Chem. B*, 1997, **101**, 9600–9605.

33 C. L. Raston, J. L. Atwood, P. J. Nichols and I. B. N. Sudria, *Chem. Commun.*, 1996, 2615–2616.

34 J. L. Atwood, M. J. Barnes, M. G. Gardiner and C. L. Raston, *Chem. Commun.*, 1996, 1449–1450.

35 (*a*) T. Drovetskaya, C. A. Reed and P. D. W. Boyd, *Tetrahedron Lett.*, 1995, **36**, 7971–7974; (*b*) Y. Sun, T. Drovetskaya, R. D. Bolskar, R. Bau, P. D. W. Boyd and C. A. Reed, *J. Org. Chem.*, 1997, **62**, 3642–3649.

36 (*a*) D. R. Evans, N. L. P. Fackler, Z. Xie, C. E. F. Rickard, P. D. W. Boyd and C. A. Reed, *J. Am. Chem. Soc.*, 1999, **121**, 8466–8474; (*b*) P. D. W. Boyd, M. C. Hodgson, C. E. F. Rickard, A. G. Oliver, L. Chaker, P. J. Brothers, R. D. Bolskar, F. S. Tham and C. A. Reed, *J. Am. Chem. Soc.*, 1999, **121**, 10487–10495; (*c*) M. M. Olmstead, D. A. Costa, K. Maitra, B. C. Noll, S. L. Phillips, P. M. van Calcar and A. L. Balch, *J. Am. Chem. Soc.*, 1999, **121**, 709–7097; (*d*) T. Ishii, N. Aizawa, M. Yamashita, H. Matsuzaka, T. Kodama, K. Kikuchi, I. Ikemoto and Y. Iwasa, *J. Chem. Soc., Dalton Trans.*, 2000, 4407–4412; (*e*) D. V. Konarev, I. S. Neretin, Y. L. Slovokhotov, E. I. Yudanova, N. V. Drichko, Y. M. Shul'ga, B. P. Tarasov, L. L. Gumanov, A. S. Batsanov, J. A. K. Howard and R. N. Lyubovskaya, *Chem. Eur. J.*, 2001, **7**, 2605–2616.

37 D. H. Hochmuth, S. L. J. Michel, A. J. P. White, D. L. Williams, A. G. M. Barrett and B. M. Hoffman, *Eur. J. Org. Chem.*, 2000, 593–596.

38 *The Porphyrin Handbook*, ed. K. M. Kadish, K. M. Smith and R. Guilard, Academic Press, New York, 1999.

39 D. M. Guldi, P. Neta and K.-D. Asmus, *J. Phys. Chem.*, 1994, **98**, 4617–4621.

40 (*a*) K. Tashiro, T. Aida, J.-Y. Zheng, K. Kinbara, K. Saigo, S. Sakamoto and K. Yamaguchi, *J. Am. Chem. Soc.*, 1999, **121**, 9477–9478; (*b*) J.-Y. Zheng, K. Tashiro, Y. Hirabayashi, K. Kinbara, K. Saigo, T. Aida, S. Sakamoto and K. Yamaguchi, *Angew. Chem., Int. Ed.*, 2001, **40**, 1858–1861.

41 D. Sun, F. S. Tham, C. A. Reed, L. Chaker, M. Burgess and P. D. W. Boyd, *J. Am. Chem. Soc.*, 2001, **123**, 10704–10705.

42 D. M. Guldi, T. Da Ros, P. Braiuca, Maurizio Prato and E. Alessio, *J. Mater. Chem.*, 2002, DOI 10.1039/b202116a.

43 (*a*) J. F. Nierengarten, L. Oswald, J.-F. Eckert, J.-F. Nicoud and N. Armaroli, *Tetrahedron Lett.*, 1999, **40**, 5681–5684; (*b*) J.-F. Eckert, D. Byrne, J.-F. Nicoud, L. Oswald, J. F. Nierengarten, M. Numata, A. Ikeda, S. Shinkai and N. Armaroli, *New. J. Chem.*, 2000, **24**, 749–758.

44 Cyclotriveratrylene-based dendritic structures revealed a trend: the association constant increases as the generation number of the surrounding dendritic substituents increased.

45 (*a*) Y.-P. Sun and C. E. Bunker, *Nature*, 1993, **365**, 398; (*b*) Y.-P. Sun and C. E. Bunker, *Chem. Mater.*, 1994, **6**, 578–580.

46 (*a*) G. V. Andriesvsky, M. V. Kosevich, O. M. Vovk, V. S. Shelkovsky and L. A. Vashchenko, *J. Chem. Soc., Chem. Commun.*, 1995, **12**, 1281–1282; (*b*) G. V. Andrievsky, V. K. Klochkov, E. L. Karyakina and N. O. Mchedlov-Petrossyan, *Chem. Phys. Lett.*, 1999, **300**, 392–396; (*c*) S. Deguchi, R. G. Alargova and K. Tsujii, *Langmuir*, 2001, **17**, 6013–6017.

47 W. A. Scrivens, J. M. Tour, K. E. Creek and L. Pirisi, *J. Am. Chem. Soc.*, 1994, **116**, 4517–4518.

48 A spherical $(C_{60})_{13}$-cluster with a diameter of 2.8 nm was shown theoretically — molecular dynamics approach — to be the smallest stable form among all possible aggregates. L. Bulavin, I. Adamenko, Y. Prylutskyy, S. Durov, A. Graja, A. Bogucki and P. Scharff, *Phys. Chem. Chem. Phys.*, 2000, **2**, 1627–1629.

49 (*a*) M. Fujitsuka, H. Kasai, A. Masuhara, S. Okada, H. Oikawa, H. Nakanishi, A. Watanabe and O. Ito, *Chem. Lett.*, 1997, 1211–1212; (*b*) M. Fujitsuka, H. Kasai, A. Masuhara, S. Okada, H. Oikawa, H. Nakanishi, O. Ito and K. Yase, *J. Photochem. Photobiol. A*, 2000, **133**, 45–50.

50 In aqueous media the cluster formation is irreversible; addition of salts (*i.e.*, osmotic effects) or surfactants did not lead to a re-transformation into the monomeric components[34].

51 V. Biju, S. Barazzouk, K. George Thomas, M. V. George and P. V. Kamat, *Langmuir*, 2001, **17**, 2930–2936.

52 K. G. Thomas, V. Biju, D. M. Guldi, P. V. Kamat and M. V. George, *J. Phys. Chem. B*, 1999, **103**, 8864–8869.

53 (*a*) P. V. Kamat, S. Barazzouk, S. Hotchandani and K. George Thomas, *Chem. Eur. J.*, 2000, **6**, 3914–3921; (*b*) P. V. Kamat, S. Barazzouk, K. George Thomas and S. Hotchandani, *J. Phys. Chem. B*, 2000, **104**, 4014–4017.

54 S. Niu and D. Mauzerall, *J. Am. Chem. Soc.*, 1996, **118**, 5791–5795.

55 (*a*) H. Murakami, M. Shirakusa, T. Sagara and N. Nakashima, *Chem. Lett.*, 1999, 815–816; (*b*) M. Sano, K. Oishi, T. Ishi-i and S. Shinkai, *Langmuir*, 2000, **16**, 3773–3776; (*c*) N. Nakashima,

T. Ishii, M. Shirakusa, T. Nakanishi, H. Murakami and T. Sagara, *Chem. Eur. J.*, 2001, **7**, 1766–1772.
56 (*a*) M. Sawamura, N. Nagahama, M. Toganoh, U. E. Hackler, H. Isobe, E. Nakamura, S.-Q. Zhou and B. Chu, *Chem. Lett.*, 2000, 1098–1099; (*b*) S. Zhou, C. Burger, B. Chu, M. Sawamura, N. Nagahama, M. Toganoh, U. E. Hackler, H. Isobe and E. Nakamura, *Science*, 2001, **291**, 1944–1947.
57 A. M. Cassell, C. L. Asplund and J. M. Tour, *Angew. Chem., Int. Ed.*, 1999, **38**, 2403–2405.
58 V. Georgakilas, F. Pellarini, M. Prato, D. M. Guldi, M. Melle-Franco and F. Zerbetto, *Proc. Natl. Acad. Sci.*, 2002, **99**, 5075.
59 K. Prassides, M. Keshavarz-K, E. Beer, C. Bellavia, R. Gonzalez, Y. Murata, F. Wudl, A. K. Cheetham and J. P. Zhang, *Chem. Mater.*, 1996, **8**, 2405–2408.
60 Z. Shi, J. Jin, Y. Li, Z. Guo, S. Wang, L. Jiang and D. Zhu, *New. J. Chem.*, 2001, **25**, 670–672.
61 (*a*) M. Hetzer, H. Clausen-Schaumann, S. Bayerl, T. M. Bayerl, X. Camps, O. Vostrowsky and A. Hirsch, *Angew. Chem., Int. Ed.*, 1999, **38**, 1962–1965; (*b*) M. Brettreich, S. Burghardt, C. Böttcher, T. Bayerl, S. Bayerl and A. Hirsch, *Angew. Chem., Int. Ed.*, 2000, **39**, 1845–1848.
62 (*a*) S. R. Wilson and Y. Wu, *J. Chem. Soc., Chem. Commun.*, 1993, 784–786; (*b*) J. Osterodt, A. Zett and F. Voegtle, *Tetrahedron*, 1996, **52**, 4949–4962.
63 (*a*) J. P. Bourgeois, L. Echegoyen, M. Fibbioli, E. Pretsch and F. Diederich, *Angew. Chem., Int. Ed.*, 1998, **37**, 2118–2121; (*b*) S. G. Liu and L. Echegoyen, *Eur. J. Org. Chem.*, 2000, 1157–1163.
64 (*a*) A. Gouloumbis, S.-G. Liu, A. Sastre, P. Vazquez, L. Echegoyen and T. Torres, *Chem. Eur. J.*, 2000, **6**, 3600–3607; (*b*) F. Hauke, A. Hirsch, S.-G. Liu, L. Echegoyen, A. Swartz, C. Luo and D. M. Guldi, *Chem. Phys. Chem.*, 2002, **2** in press; (*c*) D. M. Guldi and T. Torres, unpublished results; (*d*) N. Armaroli, G. Marconi, L. Echegoyen, J.-P. Bourgeois and F. Diederich, *Chem. Eur. J.*, 2000, **6**, 1629–1645; (*e*) D. M. Guldi, C. Luo, M. Prato, A. Troisi, F. Zerbetto, M. Scheloske, E. Dietel, W. Bauer and A. Hirsch, *J. Am. Chem. Soc.*, 2001, **123**, 9166–9167.
65 E. Sartori, L. Garlaschelli, A. Toffoletti, C. Corvaja, M. Maggini and G. Scorrano, *Chem. Commun.*, 2001, 311–312.
66 (*a*) M. V. Martínez-Díaz, N. S. Fender, M. S. Rodríguez-Morgade, M. Gómez-López, F. Diederich, L. Echegoyen, J. F. Stoddart and T. Torres, *J. Mater. Chem.*, 2002, DOI 10.1039/b110270m; (*b*) D. M. Guldi and T. Torres, unpublished results.
67 (*a*) U. S. Schubert, C. H. Weidl, P. Rapta, E. Harth and K. Muellen, *Chem. Lett.*, 1999, 949–950; (*b*) U. S. Schubert, C. Eschbaumer, O. Hien and P. R. Andres, *Tetrahedron Lett.*, 2001, **42**, 4705–4707.
68 (*a*) F. Diederich, C. O. Dietrich-Buchecker, J.-F. Nierengarten and J.-P. Sauvage, *Chem. Commun.*, 1995, 781–782; (*b*) N. Armaroli, F. Diederich, C. O. Dietrich-Buchecker, L. Flamigni, G. Marconi, J.-F. Nierengarten and J.-P. Sauvage, *Chem. Eur. J.*, 1998, **4**, 406–416.
69 (*a*) N. Armaroli, C. Boudon, D. Felder, J.-P. Gisselbrecht, M. Gross, G. Marconi, J.-F. Nicoud, J.-F. Nierengarten and V. Vicinelli, *Angew. Chem., Int. Ed.*, 1999, **38**, 3730–3733; (*b*) J.-F. Nierengarten, D. Felder and J.-F. Nicoud, *Tetrahedron Lett.*, 1999, **40**, 273–276.
70 M. Maggini and D. M. Guldi, unpublished results.
71 A. Juris, V. Balzani, F. Barigelletti, S. Campagna, P. Belser and A. von Zelewsky, *Coord. Chem. Rev.*, 1988, **84**, 85.
72 (*a*) M. Maggini, A. Dono', G. Scorrano and M. Prato, *J. Chem. Soc., Chem. Commun.*, 1995, 845–846; (*b*) D. Armspach, E. C. Constable, F. Diederich, C. E. Housecraft and J.-F. Nierengarten, *J. Chem. Soc., Chem. Commun.*, 1996, 2009–2010; (*c*) M. Maggini, D. M. Guldi, S. Mondini, G. Scorrano, F. Paolucci, P. Ceroni and S. Roffia, *Chem. Eur. J.*, 1998, **4**, 1992–2000; (*d*) D. Armspach, E. C. Constable, F. Diederich, C. E. Housecroft and J.-F. Nierengarten, *Chem. Eur. J.*, 1998, **4**, 723–733; (*e*) A. Polese, S. Mondini, A. Bianco, C. Toniolo, G. Scorrano, D. M. Guldi and M. Maggini, *J. Am. Chem. Soc.*, 1999, **121**, 3456–3452; (*f*) D. M. Guldi, M. Maggini, N. Martin and M. Prato, *Carbon*, 2000, **38**, 1615–1623; (*g*) D. M. Guldi, M. Maggini, E. Menna, G. Scorrano, P. Ceroni, M. Marcaccio, F. Paolucci and S. Roffia, *Chem. Eur. J.*, 2001, **7**, 1597–1605.
73 A gold surface and gold-nanoparticles were also probed as a template for a C_{60}–bipyridyl precursor. C. Du, B. Xu, Y. Li, C. Wang, Z. Shi, H. Fang, S. Xiao and D. Zhu, *New J. Chem.*, 2001, **25**, 1191–1194.
74 T. Haino, H. Araki, Y. Yamanaka and Y. Fukazawa, *Tetrahedron Lett.*, 2001, **42**, 3203–3206.
75 (*a*) N. Armaroli, F. Diederich, L. Echegoyen, T. Habicher, L. Flamigni, G. Marconi and J. F. Nierengarten, *New J. Chem.*, 1999, 77–83; (*b*) F. D'Souza, G. R. Deviprasad, M. S. Rahman and J.-P. Choi, *Inorg. Chem.*, 1999, **38**, 2157–2160; (*c*) T. DaRos, M. Prato, D. M. Guldi, E. Alessio, M. Ruzzi and L. Pasimeni, *Chem. Commun.*, 1999, 635–636; (*d*) T. DaRos, M. Prato, D. M. Guldi, M. Ruzzi and L. Pasimeni, *Chem. Eur. J.*, 2001, **7**, 816–827; (*e*) F. D'Souza, N. P. Rath, G. R. Deviprasad and M. E. Zandler, *Chem. Commun.*, 2001, 267–268.
76 F. Hauke, A. Swartz, D. M. Guldi and Andreas Hirsch, *J. Mater. Chem.*, 2002, DOI 10.1039/b202060b.
77 F. D'Souza, G. R. Deviprasad, M. E. El-Khouly, M. Fujitsuka and O. Ito, *J. Am. Chem. Soc.*, 2001, **123**, 5277–5284.
78 D. M. Guldi, C. Luo, T. Da Ros, M. Prato, E. Dietel and A. Hirsch, *Chem. Commun.*, 2000, 375–376.
79 D. M. Guldi, C. Luo, A. Swartz, M. Scheloske and A. Hirsch, *Chem. Commun.*, 2001, 1066–1067.
80 (*a*) A. M. Cassell, W. A. Scrivens and J. M. Tour, *Angew. Chem., Int. Ed.*, 1998, **37**, 1528–1531; (*b*) S. Takenaka, K. Yamashita, M. Takagi, T. Hatta, A. Tanaka and O. Tsuge, *Chem. Lett.*, 1999, 319–320; (*c*) S. Takenaka, K. Yamashita, M. Takagi, T. Hatta and O. Tsuge, *Chem. Lett.*, 1999, 321–322.
81 E. Nakamura, H. Isobe, N. Tomita, M. Sawamura, S. Jinno and H. Okayama, *Angew. Chem., Int. Ed.*, 2000, **39**, 4254–4257.
82 (*a*) C. Luo, D. M. Guldi, M. Maggini, E. Menna, S. Mondini, N. A. Kotov and M. Prato, *Angew. Chem., Int. Ed.*, 2000, **39**, 3905–3909; (*b*) D. M. Guldi, C. Luo, D. Koktysh, N. A. Kotov, T. Da Ros, S. Bosi and M. Prato, *Nano Lett.*, 2002, in press.
83 Y. Liu, Y. Wang, H. Lu and R. O. Claus, *J. Phys. Chem. B*, 1999, **103**, 2035–2036.
84 (*a*) H. Mattoussi, M. F. Rubner, F. Zhou, J. Kumar, S. K. Tripathy and L. Y. Chiang, *Appl. Phys. Lett.*, 2000, **77**, 1540–1542; (*b*) M. F. Durstock, B. Taylor, R. J. Spry, L. Chiang, S. Reulbach, K. Heitfeld and J. W. Baur, *Synth. Met.*, 2001, **116**, 373–377.
85 A. Ikeda, T. Hatano, S. Shinkai, T. Akiyama and S. Yamada, *J. Am. Chem. Soc.*, 2001, **123**, 4855–4856.
86 M. M. Olstead, K. Maitra and A. L. Balch, *Angew. Chem., Int. Ed.*, 1999, **38**, 231–233.
87 (*a*) R. Sijbesma, G. Srdanov, F. Wudl, J. A. Castoro, C. Wilkins, S. H. Friedman, D. L. DeCamp and G. L. Kenyon, *J. Am. Chem. Soc.*, 1993, **115**, 6510–6512; (*b*) S. H. Friedman, D. L. DeCamp, R. Sijbesma, G. Srdanov, F. Wudl and G. L. Kenyon, *J. Am. Chem. Soc.*, 1993, **115**, 6506–6509; (*c*) S. H. Friedman, P. S. Ganapathi, Y. Rubin and G. L. Kenyon, *J. Med. Chem.*, 1998, **41**, 2424–2429.